http://lib.uliege.be https://matheo.uliege.be

Representation of Foehn events in the Modèle Atmosphérique Régional (MAR) in Patagonia

Auteur : Damseaux, Adrien
Promoteur(s) : Fettweis, Xavier; Cornet, Yves
Faculté : Faculté des Sciences
Diplôme : Master en sciences géographiques, orientation climatologie, à finalité approfondie
Année académique : 2017-2018
URI/URL : http://hdl.handle.net/2268.2/5577

Avertissement à l'attention des usagers :

Tous les documents placés en accès ouvert sur le site le site MatheO sont protégés par le droit d'auteur. Conformément aux principes énoncés par la "Budapest Open Access Initiative"(BOAI, 2002), l'utilisateur du site peut lire, télécharger, copier, transmettre, imprimer, chercher ou faire un lien vers le texte intégral de ces documents, les disséquer pour les indexer, s'en servir de données pour un logiciel, ou s'en servir à toute autre fin légale (ou prévue par la réglementation relative au droit d'auteur). Toute utilisation du document à des fins commerciales est strictement interdite.

Par ailleurs, l'utilisateur s'engage à respecter les droits moraux de l'auteur, principalement le droit à l'intégrité de l'oeuvre et le droit de paternité et ce dans toute utilisation que l'utilisateur entreprend. Ainsi, à titre d'exemple, lorsqu'il reproduira un document par extrait ou dans son intégralité, l'utilisateur citera de manière complète les sources telles que mentionnées ci-dessus. Toute utilisation non explicitement autorisée ci-avant (telle que par exemple, la modification du document ou son résumé) nécessite l'autorisation préalable et expresse des auteurs ou de leurs ayants droit.

UNIVERSITY OF LIÈGE

FACULTY OF SCIENCES

DEPARTMENT OF GEOGRAPHY

Representation of Foehn events in the Modèle Atmosphérique Régional (MAR) in Patagonia

Can a change in DEM generalization improve the model?

Author
Adrien DAMSEAUX

Supervisors
Dr. X. FETTWEIS
Pr. Y. CORNET
Jury president
Dr. X. FETTWEIS
Reader
Dr. G. HOUBRECHTS

This thesis is submitted for the degree of
MASTER IN GEOGRAPHICAL SCIENCES, CLIMATOLOGY ORIENTATION

Academic year 2017-2018 Defence date: September 2018

UNIVERSITY OF LIÈGE

FACULTY OF SCIENCES

DEPARTMENT OF GEOGRAPHY

Representation of Foehn events in the Modèle Atmosphérique Régional (MAR) in Patagonia

Can a change in DEM generalization improve the model?

Author
Adrien DAMSEAUX

Supervisors
Dr. X. FETTWEIS
Pr. Y. CORNET

Jury president
Dr. X. FETTWEIS

Reader
Dr. G. HOUBRECHTS

This thesis is submitted for the degree of
MASTER IN GEOGRAPHICAL SCIENCES, CLIMATOLOGY ORIENTATION

Academic year 2017-2018 Defence date: September 2018

Acknowledgements

First, I would like to express my sincere gratitude to my two master thesis supervisors, Dr. Xavier Fettweis and Pr. Yves Cornet, who recommended me this research and assisted me throughout the whole process of this work.

I also thank Dr. Xavier Fettweis for giving me the opportunity to present my results at the EGU conference in Vienna.

I address special thanks to my friend, Loïc Lecrenier, as well as my mother, Sandra Serafini, who gave me their critical views and greatly helped me in the writing process of my master thesis.

Finally, I thank all the people who contributed in a way or another to the successful achievement of this research.

Abstract

This study focuses on the Patagonian region, where significant Foehn events are observed on both sides of the Andes throughout the whole year. These climatic phenomena are not yet well simulated by General Circulation Models (GCM) and Regional Climate Models (RCM). It has been agreed that one source of this shortcoming is related to the Digital Elevation Model (DEM) generalization, which means the generalization of the altitudes from a high-resolution DEM to a coarser resolution model grid. At low resolution, most current GCMs and RCMs use DEM generalization methods that smooth the relief, a key controlling factor in Foehn events modelling. The aim of this study is to compare three additional methods of DEM generalization (percentile 90 - P90, envelope maximum - EM, and thalweg and crests - TC methods) and evaluate their influence on simulated precipitation and temperature fields (at 10 km resolution) on the eastern part of Patagonia, where warm and dry air masses are expected. Thanks to the Modèle Atmosphérique Régional (MAR), an RCM specifically developed for polar regions, we perform three sensitivity experiments showing a significant decrease in precipitation for the P90 and EM methods and an increase in mean temperature by P90 and TC methods in our region of interest. However, the mean temperature increase and precipitation decrease are not sufficient to cope with the biases observed with the Climate Research Unit (CRU) gridded climate datasets. We conclude that none of these three methods are perfect and present different strengths and weaknesses. This study serves as a recommendation for a better representation of Foehn events and a better use of DEM generalization to existing climate models performing in Patagonia but also for regions sharing the same orographic features as the Patagonian relief.

Résumé

Cette étude se concentre sur la Patagonie, où d'importants événements Foehn sont observés des deux côtés des Andes tout au long de l'année. Ces phénomènes climatiques ne sont pas encore bien simulés par les General Circulation Models (GCM) et les Regional Climate Models (RCM). Il a été convenu que l'une des sources de ce manque est liée à la généralisation du modèle numérique d'élévation de terrain ou Digital Elevation Model (DEM), qui consiste en une généralisation des altitudes d'un DEM à haute résolution à une grille à plus basse résolution. À basse résolution, la plupart des GCMs et des RCMs actuels utilisent la méthode de généralisation du DEM qui lisse le relief, un facteur de contrôle clé dans la modélisation des événements de Foehn. Le but de cette étude est de comparer trois méthodes originales de généralisation du DEM (percentile 90 - P90, envelope maximum - EM, et thalweg et crests - TC methods) et d'évaluer leur influence sur les champs simulés de précipitations et de températures (à 10 km de résolution) sur la partie est de la Patagonie, où des masses d'air chaud et sec peuvent être observées tout au long de l'année. Grâce au Modèle Atmosphérique Régional (MAR) , un RCM développé spécifiquement pour les régions polaires, nous réalisons trois expériences de sensibilité montrant une diminution significative des précipitations pour les méthodes P90 et EM et une augmentation de la température moyenne par les méthodes P90 et TC dans notre région d'intérêt. Cependant, l'augmentation de la température moyenne et la diminution des précipitations ne sont pas suffisantes pour faire face aux biais observés dans les ensembles de données climatiques quadrillés du Climate Research Unit (CRU). Nous concluons qu'aucune de ces trois méthodes n'est parfaite et présente des forces et des faiblesses différentes. Cette étude sert de recommandation pour une meilleure représentation des événements de Foehn et une meilleure utilisation de la généralisation du DEM aux modèles climatiques existants fonctionnant en Patagonie mais aussi pour des régions partageant les mêmes caractéristiques orographiques que le relief patagonien.

Contents

List of Figures

Chapter 1

Introduction

1.1 Motivations and research context

Due to its orographic, geographical and climatic situation, Patagonia is often mentioned as an ideal region to study Foehn events (Smith and Evans, 2007). The Andes mountain range is high, narrow and perpendicular to the main winds coming from the oceans. All the parameters are met to observe both highly pronounced upslope rains and the rain shadow effect (explained in details in Chapter 2) on the western and eastern side of the mountains, respectively, throughout the year. These two typical characteristics have huge consequences on the region, separating it into two types of climates with their distinct biomes. The mountain divides wetland vegetation areas in the western part from drier vegetation areas in the eastern part.

Because of its complex orographic features, the Foehn events in Patagonia have always been difficult to represent in climate models. At present time, there have been a few studies for providing high-resolution climate simulations at the regional level using Regional Climate Models (RCMs) over Patagonia (Solman et al. 2013; Garreaud et al. 2013; Lenaerts et al. 2014; Villarroel et al. 2013). These studies have privileged RCMs over General Circulation Models (GCM) because the spatial resolutions of GCMs are too coarse to accurately simulate events like Foehn effect in our region of interest (Seluchi et al. 2003 ; Klink 1995). Most of these efforts highlight the orographic precipitation modelling deficiency in actual RCMs and GCMs and its relation with the surface elevation model.

To resolve this shortcoming, a common method used in the literature is to enhance the spatial resolution of the model to retrieve a finer and more complex surface elevation, at the expense of calculation time and/or surface area covered. This technique turned out to be successful in a large number of studies, in Patagonia (Lenaerts et al., 2014) but also in other regions over the world like in Greece (George et al., 2012), in Antarctica (Andrew et al., 2014), or in USA (Wehner et al., 2010).

1.2 Aim of our research

This master thesis tackles the problem of Foehn events modelling in Patagonia from a different angle than by refining spatial resolution. We address the concept of digital elevation model (DEM) generalization, which means the generalization of spatial data (e.g. surface altitude) at a resolution coarser than the collected resolution provided by high-resolution models.

The aim of our study is twofold. First, different preselected DEM generalization methods are assessed to evaluate their ability to aggregate a common high-resolution DEM, ETOPO1 (Amante and Eakings, 2009), at low-resolution in the Patagonian region. The second objective is to understand how DEM generalizations influence climate models. The Modèle Atmosphérique Régionale (MAR) developed at the University of Liège is therefore used to simulate sensitivity experiments using outputs of several generalization methods of ETOPO1 over the 2002-2016 period.

We work on the hypothesis that a change in the orographic generalization method of a climate model can help us better represent the climate in Patagonia at low resolution.

1.3 Research plan

After this introduction, the second chapter of our study presents the state of the art including an overview of the Patagonian climate, of Foehn winds and of the previous RCMs simulations performed in the region. Our hypothesis is then introduced.

After that, we define DEM generalization and describe the existing research on this concept in the third chapter. In addition, the methodology and a comparison of additional methods implemented in our study are discussed.

The fourth chapter evaluates the influences of DEM generalization on climatic variables by conducting three DEM generalization sensitivity experiments. The model inputs, outputs, the validation as well as the set-up and forcings used in MAR simulations are also discussed.

We conclude our research in the fifth chapter with some perspectives for further studies.

Finally, a list of acronyms used in the following chapters is listed at the end of this thesis.

Chapter 2

State of the art and hypothesis

Patagonia, the region of our study case, is a wide and diverse region. Figure 2.1 shows a topographic map of the region. Its range extends from the southern part of South America at about 40°S down to the southern tip of the continent at about 55°S. The southern portion of the Andes divides the narrow and orographically higher Chilean Patagonia, from the lower Argentinian Patagonia extending for several hundred kilometres to the Atlantic Ocean. The Andes are the most important mountain range in the Southern Hemisphere. In Patagonia, mean height reaches about 1500 m, but many peaks are in excess of 3000 m. In contrast with altitude, the longitudinal extent of the mountain is comparatively narrow (less than 200 km). Due to impressive length, continuity and height, Garreaud (2009) states that the mountain chain significantly interferes with the atmospheric circulation, resulting in a variety of climate patterns and synoptic scale phenomena.

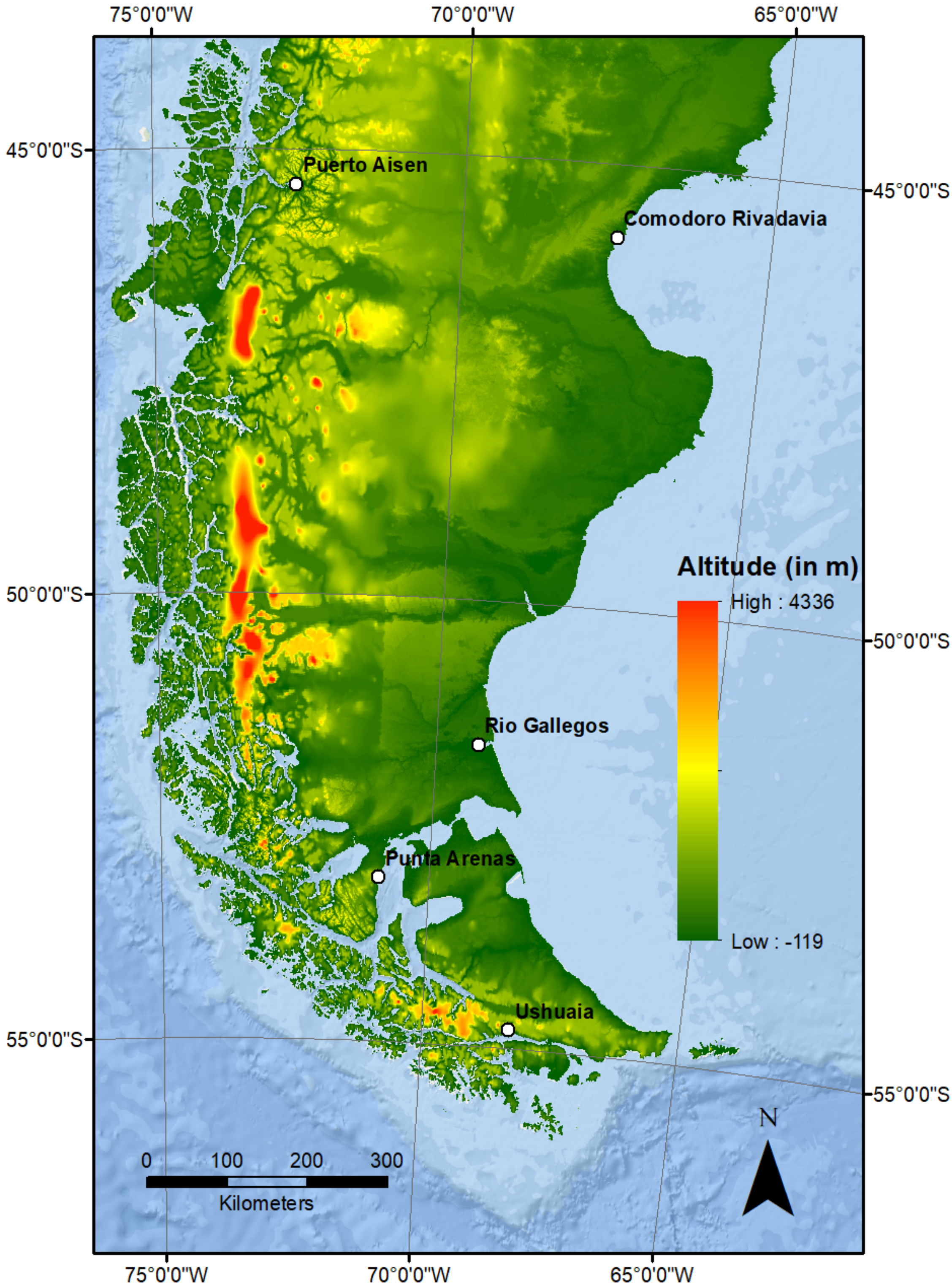

Figure 2.1 Topography of Patagonia derived from GLOBE Task Team, eds., 1999. The coordinate projection is an azimuthal Postel oblique with a central meridian at 74°W and a latitude of origin at 47°S. White points represent some major cities in the region.

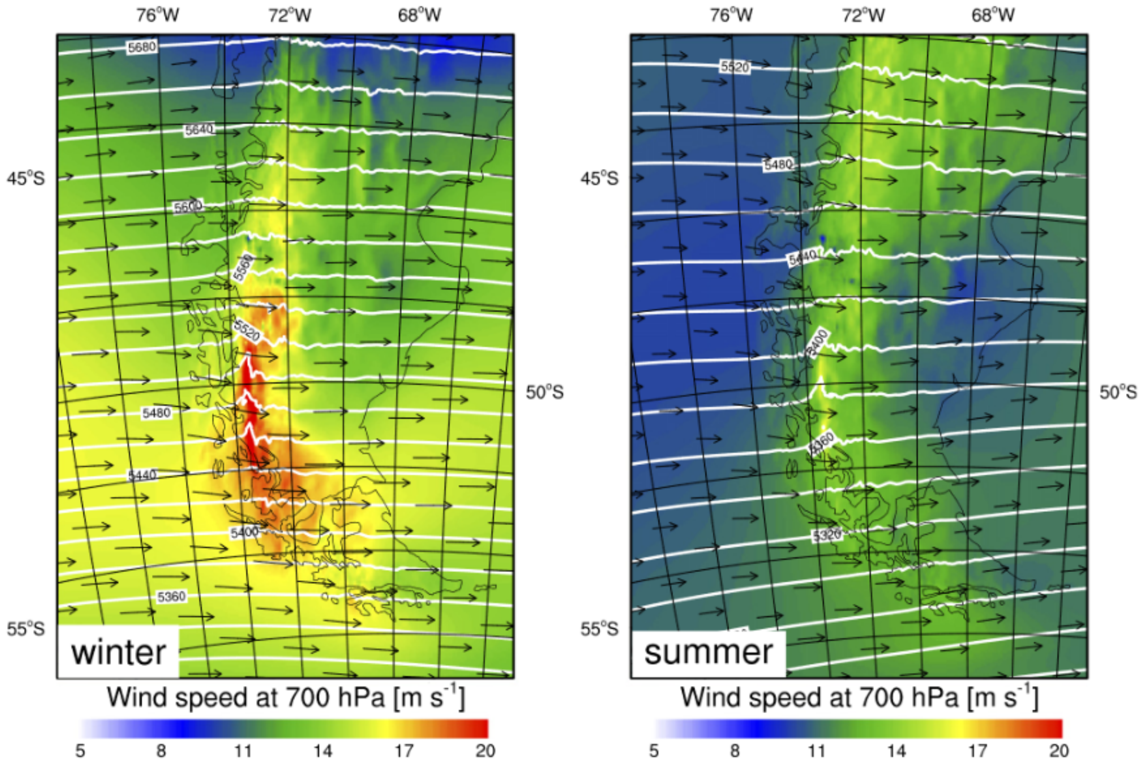

Figure 2.2 Simulated (left) winter (June–August) and (right) summer (December–February) wind speed (colors), direction (arrows), and geopotential height (white lines, dam) at 700 hPa over the 1979-2012 period in Patagonia. Retrieved from Lenaerts et al. (2014).

2.1 Climate pattern

The region is characterized by two types of climates (Paruelo et al. 1998; Garreaud et al. 2013; Seluchi et al. 2003). The Andes divides the wetter western part from the drier eastern part. It can be explained by the crucial role of the mountain acting as an orographic barrier and blocking the cold and wet eastern air masses from the Pacific Ocean (Seluchi et al. 2003) displayed on figure 2.2. This blocking effect has a huge influence on the Patagonian climate and is often mentioned as an excellent "laboratory" to study Foehn events (Smith and Evans 2007). First, it is responsible for the strong warm and dry winds, called Foehn winds, descending from the mountains towards the eastern valleys throughout the whole year. Secondly, the combined influence of the winds from the Pacific Ocean and the orographic barrier perpendicular to these winds result in a strong west-easterly gradient of precipitation across the entire region (Lenaerts et al. 2014; Viale and Garreaud 2015; Berman et al. 2012).

According to Garreaud et al. (2013), annual rainfall can exceed 5000 - 10,000 mm on the western part due to the fast orographic rising air masses, whereas the mean precipitation decreases to less than 300 mm a year just a few tens of kilometres downstream and only reaches 500 to 700 mm a year close to the Atlantic coast. This aridity is generally related to the term "rain shadow effect" (Jacques-Coper et al. 2015). Paruelo et al. (1998) says the role of the mountain is so important that the distance of a region from it can explain 94% of the spatial variability of the mean annual precipitation.

Patagonian climate is also driven by both the semi-permanent anticyclones of the Pacific and the Atlantic oceans, situated at approximately 30°S, and the sub-polar low pressure belt, situated at approximately 60°S (Lenaerts et al. 2014; Berman et al. 2012). The precipitation pattern is influenced by the seasonal movement of these low and high pressure systems. For example, it explains the main inter-annual variability of precipitation in the region. In winter, the combination of the intensification of the sub-polar low, the northern displacement of the Pacific high and the higher difference of oceans and continental temperatures leads to an increase in precipitation compared to the summer situation (Smith and Evans 2007; Paruelo et al. 1998; Quintana and Aceituno 2012; Garreaud et al. 2013). However, some studies (Garreaud 2013; Garreaud et al. 2013; Lenaerts et al. 2014) have observed higher precipitation in the summer in the western region, close to the ridges. Lenaerts et al. (2014) analyses this discontinuity as a direct consequence of the heavy episodic nature of extreme precipitation events in the early 2000s.

On the western side of Patagonia, the temperature patterns exhibit a temperate or cool-temperate region (Jacques-Coper et al. 2015; Paruelo et al. 1998). While the eastern side presents a continental climate, along with a high annual thermal amplitude (Garreaud et al. 2013; Jacques-Coper et al. 2015). Berman et al. (2013) state that temperature variability has a clear separation north-south in summer and autumn with higher continental heating. Moreover, Bianchi et al. (2016) stipulate that mean temperature generally decreases when altitude increases, while in some cases the temperature can locally increase because of stable and cold air masses producing inversion in the boundary layer.

The western part presents extremely windy conditions associated with the winds descending from the mountains (Garreaud et al. 2013; Jacques-Coper et al. 2015). Carrasco et al. (2002) have noted that the winds are generally weaker in winter, with a south-westerly direction compared to summer, when the wind regime becomes stronger with a north-north-westerly direction.

The region is also significantly affected by the El Niño - Southern Oscillation and the Antarctic Oscillation, which strongly influences precipitation and temperature patterns over wide areas of Chile and Argentina, with a high temporal instability (Lara et al. 2005; Lopez et al. 2010; Silvestri and Vera 2003; Garreaud 2009).

We can also note that, according to Carrasco et al. (2002), recent studies indicate that a generalized retreat of glaciers is occurring along the Andes mountains, particularly in the Southern Patagonian ice field.

To summarize, Patagonia is separated into two climates mainly controlled by the Andes: a colder and wetter western part with a large inter-annual variation in precipitation and a hotter and drier eastern part with a large annual thermal amplitude. To that, we should also add the spatial increase of temperature in the higher latitudes and of precipitation in higher altitudes. Figure 2.3 shows the temperature and precipitation annual patterns of the region described above.

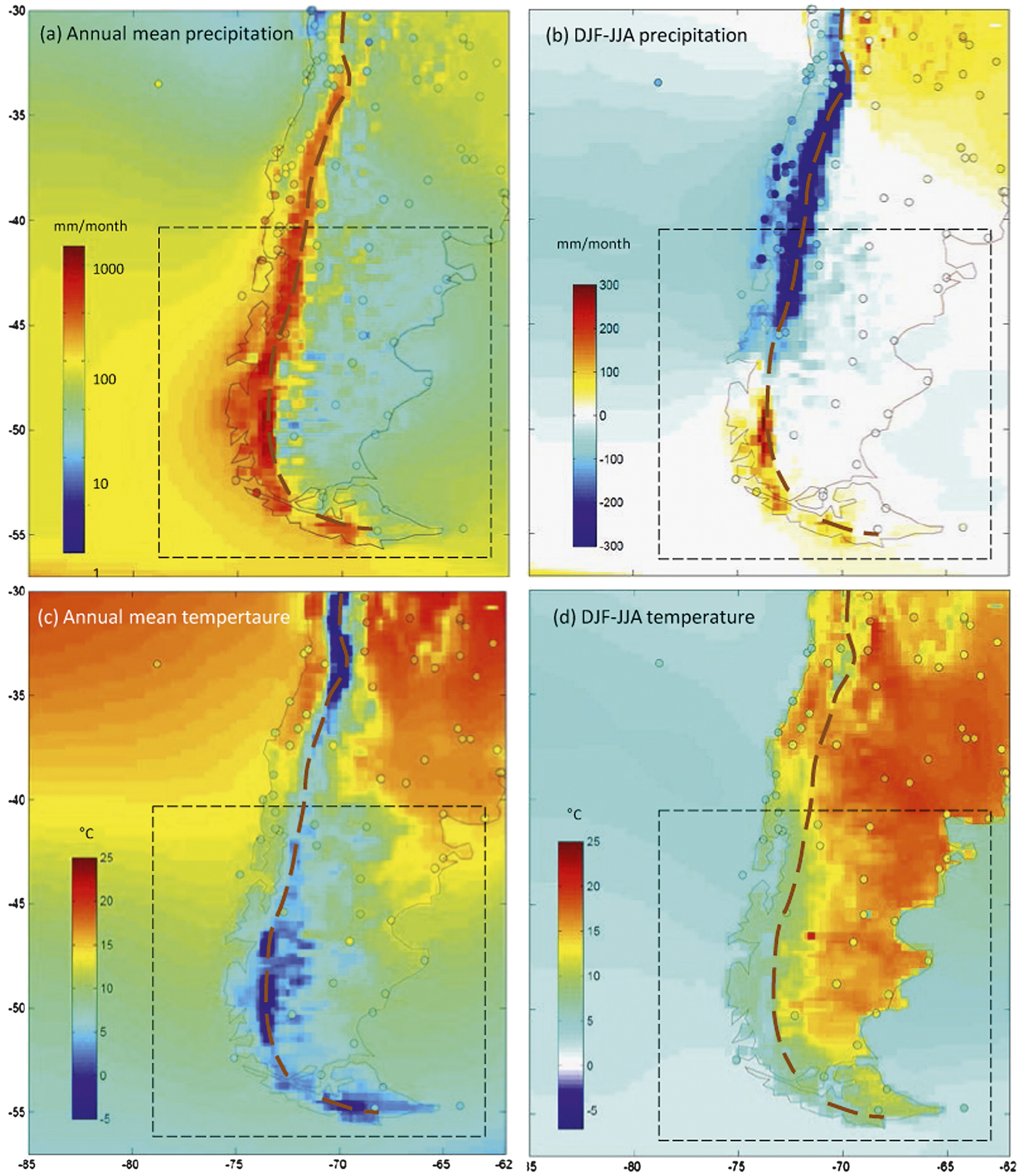

Figure 2.3 Temperature and precipitation annual patterns in Patagonia retrieved from Garreaud et al. (2013). The model climatology is computed using the period 1978–2001; the station climatology is calculated using all available monthly data during the second half of the twentieth century. (a) Annual mean precipitation; note the logarithmic colour scale. (b) Austral summer (DJF) minus winter [June – August (JJA)] mean precipitation. (c) Annual mean near-surface air temperature (1.5 m in the model; approximately 2 m in observations). (d) Austral summer (DJF) minus winter (JJA) mean near-surface air temperature.

2.2 "Foehn" winds and mechanisms

As explained by Seluchi et al. (2003), the specific warm, dry winds coming down the lee slopes get different names depending on their localisation: "Foehn" in central Europe (the name used in this study) or "Zonda" in southern America, our study region. The Foehn winds are generally discernible mainly by increases in temperature and decreases in relative humidity, and influence multiple synoptic variables (Hoinka 1985). Concerning the wind speed, it rapidly decreases with increasing lee-side distance from the baseline of the barrier. As previously stated, Foehn winds are responsible for two main events in Patagonia; the upslope rains and the rain shadow effect on the western and eastern part, respectively.

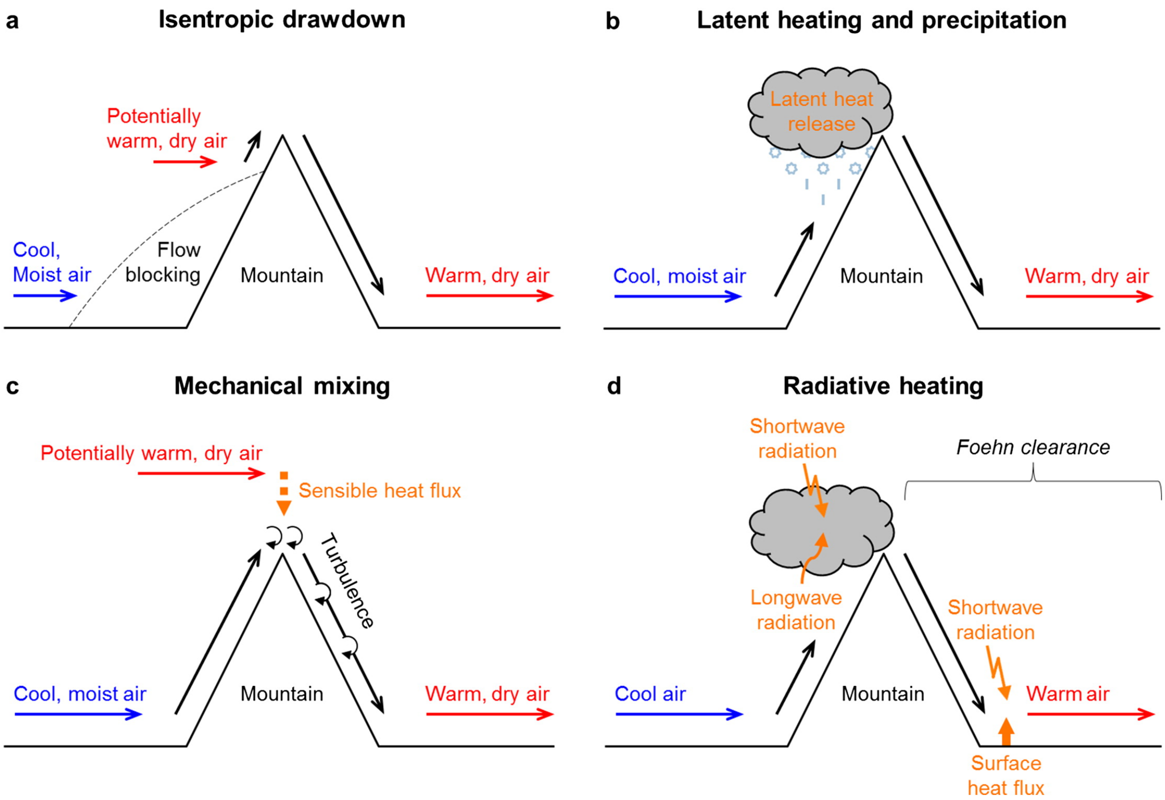

Figure 2.4 Foehn warming mechanisms retrieved from Elvidge and Renfrew (2016).

Any commonly agreed genesis mechanisms do explain the meteorological paradigm of Foehn winds. Elvidge and Renfrew (2016) summarize the four main mechanisms, as shown in Figure 2.4, widely discussed in the literature. The first mechanism called "isentropic drawdown mechanism" states that cool, moist air can be blocked upwind of the mountain. Warmer, drier air is therefore allowed to be advected isentropically (without change of entropy) from the top of the mountains to the valleys. The second is the popular "latent heating and precipitation mechanism" based on a thermodynamical Foehn theory. According to the latter, the lift of an air mass ahead of an orographic barrier leads to an increase of dry-adiabatically cooling until reaching saturation. This effect causes condensation, cloud formation, and subsequently precipitation, moisture removal of the air mass and irreversible latent heating. The resulting air mass descending to the valleys is therefore warmer and drier. These two mechanisms have been prioritized in recent years at the expense of two other still reliable Foehn mechanisms (Elvidge and Renfrew 2016; Richner and Hächler 2013). The first one, third in our list, the "mechanical mixing mechanism" implies a mechanical mix of cold, moist air passing over the mountain with potentially warmer and drier air. This mix contributes to a turbulent sensible heat and moisture flux and results in warmer, drier air descending the lee slopes. This mechanism is firstly described in Scorer (1978). Finally, the last "radiative heating" mechanism describes an atmosphere where cloud can be found on the upwind slopes and clear, dry air can be found on the downwind slopes, the "Foehn clearance". This situation encourages radiative flux convergence and thus warmer air on the lee-side.

In one of the rare quantitative investigations, Elvidge and Renfrew (2016) have demonstrated the importance of three out of these four physical mechanisms (Latent Heating, Mechanical mixing and Isentropic drawdown). The weight of each mechanism depends upon the meteorological conditions and orographic characteristics of the region. It is important to note that in these four mechanism theories, the relief is a key controlling factor.

2.3 RCMs over Patagonia

In this subsection, we review the model validation and analysis made in several recent studies on climate atmospheric modelling in Patagonia, especially in high-resolution regional climate models.

First, a large consensus of scholars (Garreaud et al. 2013; Lenaerts et al. 2014; Bianchi et al. 2016) instinctively senses that, like many other sparsely populated regions, the Patagonian region holds a small meteorological network with a low spatial density and short record length to properly describe climate variability and verify climate models. This limitation is increased by the fact that Patagonia is characterized by complex spatial patterns in precipitation and temperature. Nevertheless, Bianchi et al. (2016) state that a possible and common approach to overcome this limitation is to use gridded climate datasets, that will be discussed later.

Solman et al. (2013) present a validation of seven regional climate models at a 50 km resolution not exclusively in Patagonia but, for the whole South America continent. Like the following studies, they mainly focus on the evaluation of seasonal mean precipitation and near-surface temperature. They use several climate datasets including the Climate Research Unit (CRU) to verify the model outputs. Concerning our region of interest, they note a systematic underestimation (over 1-2°C) of the mean temperature and a large overestimation of precipitation. They also point out that the quality of observations over areas with complex orography is critical for evaluating model performance. Consequently, the model bias found in the study over Andean areas in Patagonia should be interpreted with care.

Garreaud et al. (2013) use a 25 km resolution regional atmospheric climate model to investigate the dependence of Patagonia's precipitation and near-surface air temperature on large-scale circulation anomalies during the 1978-2001 period shown in figure 2.3. The validations show an overestimation by a factor of 2 of the mean precipitation at high altitudes. However, the authors claim that the annual mean and seasonal amplitude of the surface air temperature are well simulated by the model. Nevertheless, their results show a significant underestimation of 0.5 to 1 °C during the last years of the simulations, with an increase at the end of the time series.

Another study by Lenaerts et al. (2014) uses a high-resolution (5.5 km) regional climate model to describe the present-day (1979–2012) climate of Patagonia, with a particular focus on the surface mass balance of the Patagonian ice fields. Using only three stations, the validations show a model bias (0 to -2°C) in all seasons and a clear overestimation of the precipitation in the western side of the Andes. However, the model better resolves the strong drying eastern region. In their study, the authors also underline some prospects about climate modelling in Patagonia. On the one hand, the narrow mountain range is poorly resolved in low-resolution GCMs and atmospheric reanalysis products, like ERA-Interim. On the other hand, the main advantage of this high-resolution model is the ability to reproduce a sharper surface elevation and related orographic precipitation, a feature that, they claim, is absent in the state of the art of climate models.

Villarroel et al. (2013) present a validation of a high-resolution (5 km) regional atmospheric climate model over the Northern Patagonia Ice field for the 2000-2010 period. Using twelve stations, they state that the model is able to simulate the annual mean temperature values. However, the annual thermal amplitude is lower than the observational data because temperatures are colder for summer and warmer for winter. They also note that NCAR/NCEP reanalysis shows a general colder environment in continental areas year-round compared to the observed data. Concerning the precipitation, the authors observe an overestimation of the annual precipitation up to a factor of 2. Furthermore, they believe that the inter-annual variability is well simulated by the model. In the footsteps of Lenaerts et al. (2014), this study also emphasizes the correlation between orography and precipitation amount. The researchers concluded that the model at high-resolution is a clearly better fit for air temperature and precipitation simulations because the representation of the relief is close to reality. Nevertheless, the overestimation of the precipitation and underestimation of the annual amplitude of the air temperature still need to be addressed.

In summary, some trends clearly emerge from these studies. First, there is a common overestimation of the annual mean precipitation, an underestimation of the annual amplitude of the temperature and, in some studies, an underestimation of the annual mean temperature over the whole region. It should be noted that if the precipitation bias is mostly discussed in the high altitudes because of the large absolute amounts, questions about the relative precipitation in the eastern part were not addressed. All studies definitely underline the unambiguous correlation between better relief representation in finer resolution model and associated orographic precipitation.

2.4 Goal of the research

Firstly, much attention has been focused on the modelling of precipitation in high altitude Patagonian areas, whereas there has been little concern about the consequences of Foehn winds in the eastern part. The blocking effect caused by the Andes not only increases western precipitation but also decreases eastern precipitation. Following the previous comments, an excellent representation of the relief in surface elevation model is critical to represent both effects.

Secondly, while most of the recent studies have looked at a refinement in spatial resolution, our research will focus on a crucial step in climate modelling, the DEM generalization, to address this problem.

In light of the conclusions and analyses from previous papers, the aim of our study is twofold. First, the generalization methods are assessed to estimate their ability to generalize complex relief from a common high-resolution to a low-resolution grid in the same region. Secondly, the objective is to understand how relief generalization influences climate models. Finally, we work on the hypothesis that a change in relief generalization method in a climate model can help us better represent the climate in Patagonia at low-resolution. It should be noted that our study mainly focuses on modelling the eastern warm and dry air masses.

Chapter 3

DEM generalization in Patagonia

We mentioned in Chapter 2 that the core of our hypothesis lies in the DEM (Digital Elevation Model) generalization processes. Since the data used is the surface elevation, we use the name "DEM generalization" for this method. A DEM is a regular square-grid representation of a surface elevation created from a terrain's elevation data (Wilson and Gallant, 2000). It should be pointed out that the terminology "model" is applied in the DEM literature, while it differs from the terminology "model" used in climatology. Climate models use numerical and quantitative methods to simulate the different climate drivers, whereas DEMs mostly use remote sensing and direct survey data to retrieve a surface relief.

Other terms than DEM generalization can be found in hydrological literature such as "surface elevation aggregation", "DEM aggregation", "up-scaling" or "DEM resampling". The following chapter outlines the definition of this term, the previous research in this topic, the additional methods implemented in our study and their influences on the surface relief retrieved.

3.1 Definition

Regional and global climate models need to group, or to aggregate, spatial data, e.g. altitudes, at a resolution coarser than the collected resolution provided by high-resolution models like DEM (Bian and Butler, 1999). These processes can be commonly called generalization and can be performed in different statistical and geometrical methods. Figure 3.1 shows a schematic representation of the translation from a high- to a low-resolution grid using the maximum as statistical parameter. In this thesis, we tackle the generalization of the relief, which is, as explained by Seluchi et al. (2003), a main performance-driven variable in Foehn winds modelling. This generalization is commonly called DEM generalization.

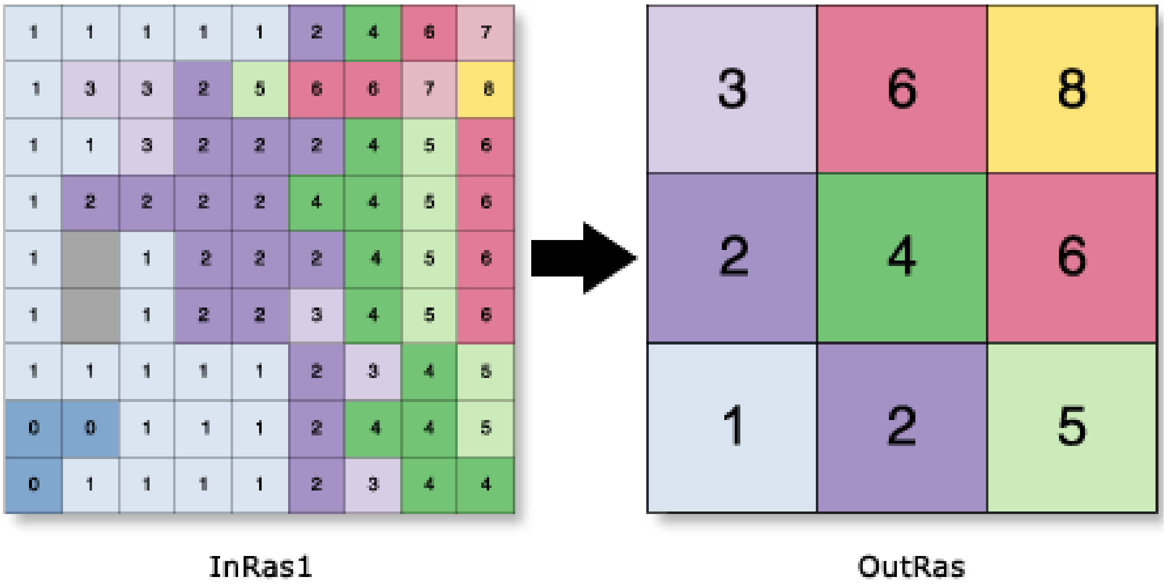

Figure 3.1 Schematic representation of a DEM generalization from high- to low-resolution grid using the maximum as statistical parameter. Adapted from ArcGIS for Desktop Basic: Requires Spatial Analyst (http://desktop.arcgis.com/en/arcmap/10.3/tools/spatial-analyst-toolbox/aggregate.htm).

3.2 Previous research

It is interesting to note that, in our investigations, few studies tackle the problem of DEM generalization and most of them are related to geomorphological research rather than to climatology.

Bindlish and Barros (1996) review three existing mathematical descriptions of relief generalization in DEM. Firstly, (i) the "mean orography method" consists in sampling DEM data through a box blur using the mean as statistical parameter. The mean value of the high-resolution pixels is assigned to the homologous low-resolution pixel. This method, which can also be referred to Vieux (1993), preserves the total volume of orographic features at the expense of the amplitude of high frequencies, which means it smoothes peaks and valleys.

A similar one (ii) "envelope orography method" consists in adding a multiple of the local standard deviation of the high-resolution DEM to the mean orography. Although this method captures topographic peaks better than the corresponding mean orography, low elevation areas such as plains and valleys are not well resolved, and the total volume of orographic features is not maintained. Figure 3.2 shows a schematic representation of pros and cons of these last two methods. It should be noted that Bindlish and Barros (1996) use the name "envelope" for the last method. However, due to the ambiguity with geomorphological terms, we call it "standard deviation box method". Finally, (iii) the Cressman-type objective analysis interpolates the altitudes on a low-resolution grid by a specific weighted function depending on the user-specified radius of influence and on the distance between the low-resolution pixel where the elevation is being computed and the high-resolution pixels in the neighbourhood. Bindlish and Barros (1996) emphasize different limitations of this method including the lack of consistency among generalization levels. They have also added their own method which consists of a modified fractal interpolation scheme. After comparing these four different methods in a study case with a DEM in California, they conclude that the last one better preserves the spatial structure of the orographic gradients.

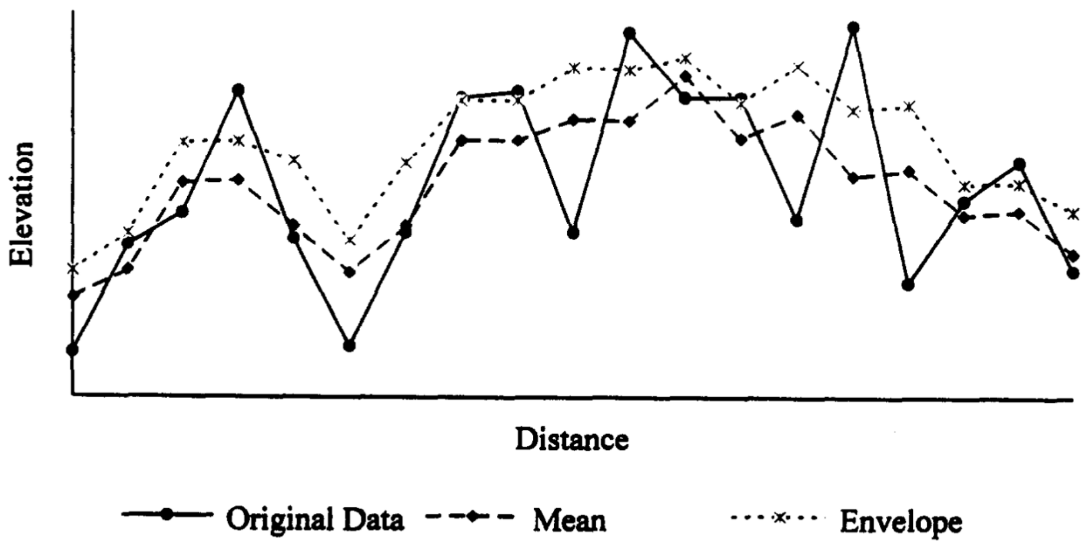

Figure 3.2 Schematic representation of orographic generalization by mean and envelope orography retrieved from Bindlish and Barros (1996). The envelope method captures orographic peaks better than the corresponding mean method. Yet, low elevation areas such as plains and valleys are not well resolved, and the total volume of orographic features is not preserved.

Bian and Butler (1999) identify a lack of systematic comparison between generalization methods. They therefore evaluate three methods using simulated images: averaging (mean method), median (using the median instead of the mean as statistical parameter) and central pixel resampling. The central pixel resampling assigns the value of the central pixel of the high-resolution window to the corresponding single low-resolution pixel.

In Le Coz et al. (2009), the authors assess an appropriate method which degrades the spatial resolution of a DEM in order to compute the water balance of the Lake Chad basin. They distinguish two kinds of algorithms: on the one hand, interpolation methods such as bilinear interpolation or cubic convolution, and on the other hand, statistical or geometrical methods such as mean, nearest neighbour (e.g. central pixel resampling), median or modal (not for elevation purpose), maximum (to preserve crests) or minimum (to preserve valleys) methods. By comparing six different operators (maximum, mean, median, minimum, mode and nearest neighbour) in their study case, they conclude that mean and median methods produce the representations of the relief that are closest to the reality.

Wu et al. (2008) select and compare three DEM resampling techniques, nearest neighbour resampling, bilinear interpolation and cubic convolution, with different DEM resolutions for two small catchments located inside Back Creek Watershed in South-West Virginia. In the cubic convolution technique, the output cells value is computed by fitting a smooth surface to the nearest 16 input cells using third order equations. It tends to smooth data even more than the bilinear interpolation. They come to the conclusion that the DEM resolution opted for the output has a more important impact on the result than the DEM resampling method used.

We note an evident lack of consensus between the nomenclature and distinctions of most generalization methods. As a consequence, we propose here a common classification of the eleven generalization methods retrieved from the literature on the domain. It is important to note that each of these methods do not refer to a fixed definition and their algorithm and application scope can differ. Nevertheless, generalization methods can be classified in two main categories.

First, the box methods category uses a box blur, a window derived from the finer resolution DEM corresponding to a pixel in the coarser resolution image (output image). The value of the latter is set to a statistical parameter of the neighbouring pixels in the finer resolution image (input image). A large amount of statistical parameters exist and have been intensively used in the literature such as (1) the mean, (2) the standard deviation (mean combined to a factor of the standard deviation), (3) the maximum, (4) the minimum, (5) the nearest neighbour resampling, (6) the median, (7) the mode or (8) the Cressman-type objective analysis.

The second category gathers all the other generalization methods whose algorithmic core does not involve a box blur. This includes (9) fractal interpolation methods, (10) cubic convolution methods and (11) bilinear interpolation.

Finally, previous scholars (Wu et al. 2008; Le Coz et al. 2009; Vieux 1993) have highlighted that the suitability of generalization methods strongly depends on the orography of the study area. In other words, the effectiveness of the method varies according to the orographic specificities of the studied region.

3.3 Current use in RCMs and GCMs

After reviewing the scientific literature, we have noticed that few climate research have tackled DEM generalization methods. It is therefore interesting to investigate which method is implemented in current GCMs and RCMs. Most models have incomplete surface elevation generalization method documentation and it is very complicated to retrieve which generalization method is used. However, a common practice, better documented, is the use of a post-treatment application to the aggregated output DEM called filter. The purpose of the latter is to add an additional smoothing of the high frequencies.

Most current GCMs are using a similar approach to the mean box method. The ECMWF model (from the European Centre For Medium Range Weather Forecasting) is coupled with a band pass filter. The latter is obtained by using a specific smoothing operator detailed by ECMWF (2003). The relief generalization used in the Global Forecast System (GFS) model of the United States' National Weather Service (NWS), which can be found in Hong (1999), is similar to the standard deviation box method.

Regarding the RCMs, there are many various and different models with incomplete DEM generalization method documentation. In our understanding, most of them use a method close to the standard deviation box in combination with a specific filter. For example, RACMO 2.0 uses a Raymond filter which takes out the variance of the pixels altitude and reduces peaks amplitude (Lenderink and Lenderink, 2003). IPRC-RegCM uses a simple standard deviation method without filter (Wang et al., 2003). Finally, MAR, the RCM used in our study, is coupled with a mean box method and a filtering of the edges of the DEM.

3.4 Study area

Our study focuses on the analysis of Foehn events in the Patagonian region. Consequently, the analysed spatial domain, shown in figure 3.3, includes two areas with, respectively, a 20 and a 10 km spatial resolution. They are wide enough to cover the whole southern tip of South America and part of the Pacific Ocean where the main winds are coming from.

The two integration domains include 80x80 pixels and 130x160 pixels for the 20 and 10 km resolution, respectively. For the coarser resolution, the upper left corner is at 39°3'S 84°3'W and the lower right is at 54°S 60°5'W. The finer resolution has an upper left corner at 39°3'S 79°2'W and a lower right at 54°S 62°9'W. The common coordinate projection used is an azimuthal Postel oblique with a central meridian at 74°W and a latitude of origin at 47°S.

As illustrated in figure 3.3, the areas cover a slightly different zone depending on their resolution. The aim is to preserve as much of the 20 km low-resolution domain while ensuring a rapid computing time, as a finer resolution means a slower calculation time.

In our research, the high-resolution DEM used is the 1 arc-minute resolution global relief model of Earth's surface, ETOPO1. The complete documentation of this DEM can be found in Amante and Eakings (2009).

3.5 Additional methods implemented in this study

The aim of this research is not only to observe the performance of DEM generalization methods listed in the literature but also to propose new kinds of algorithms specially designed for region sharing the same orographic features as Patagonia. As stated earlier, the relevance of a generalization method strongly depends on the orographic characteristics of the study area. In our case, Patagonia shows both high peaks interspersed with deep valleys in a very narrow mountain range. The output surface elevation therefore needs to keep the amplitude of these high frequencies. Furthermore, the mountain ridge is a really important orographic feature to represent because it induces the blocking effect of Foehn winds.

In addition to the former box mean method used in MAR, we have developed three additional original algorithms for DEM generalization: (i) the percentile 90 method, (ii) the envelope maximum method and (iii) the thalwegs and crests method. Details of the additional

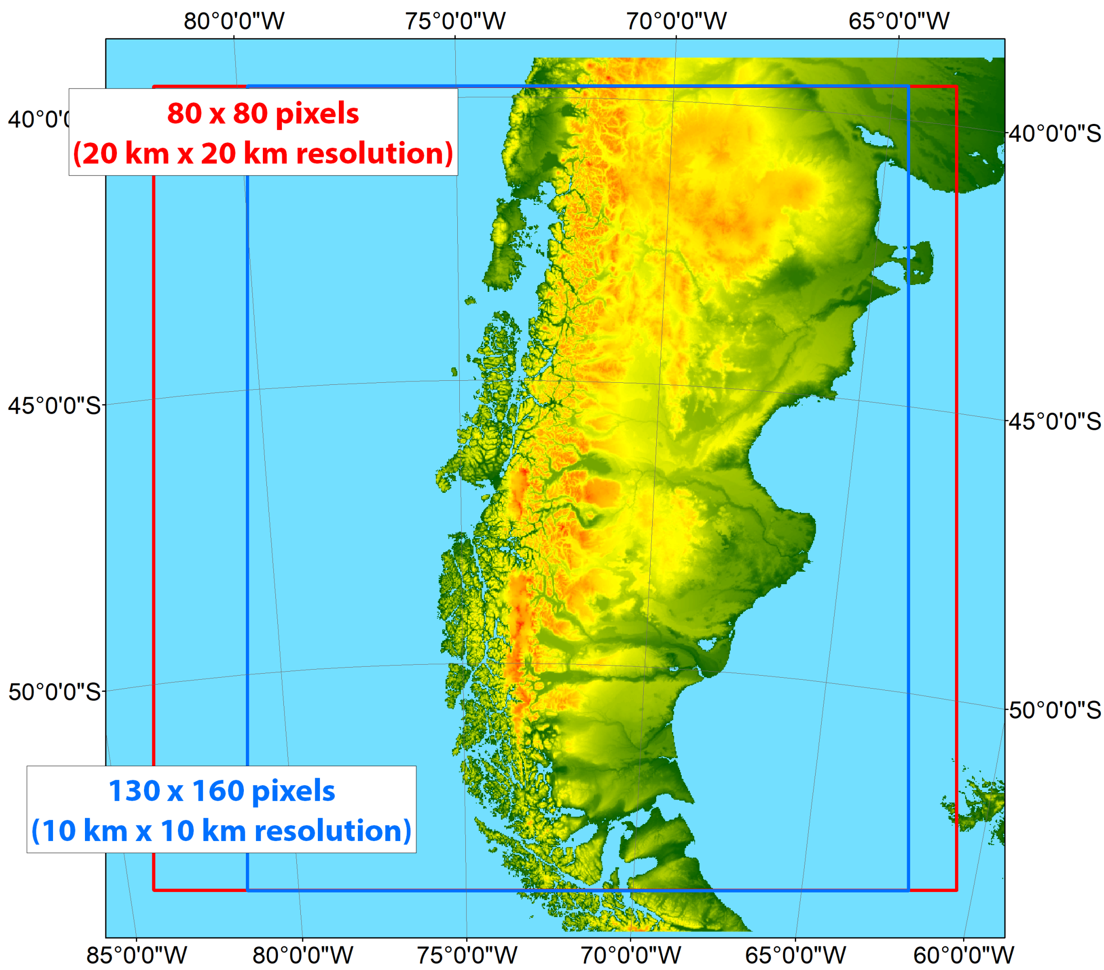

Figure 3.3 The two domains used in our study. The red rectangle represents the domain with the 20 km coarser resolution. It includes 80x80 pixels. The blue rectangle represents the 10 km finer resolution. It includes 130x160 pixels. The palette represents the surface elevation of ETOPO1, the input DEM used in our study (see Amante and Eakings (2009) for the complete documentation).

methodology methods, their influence on DEM, their pros and cons are discussed below. The former filtering of the borders in MAR is still conserved in all generalizations.

3.5.1 Methodology

(i) Percentile 90 method (P90 method)

The P90 method consists of a box method, as explained earlier, using the percentile 90 as statistical parameter. Percentile 90 is chosen to keep a maximum of high altitudes for each box blur. The aim is to preserve the mountain range without over-smoothing the valleys.

(ii) envelope maximum method (EM method)

The aim of this method goes further than the previous one by retaining to a large extent the high altitudes at the expense of, as we will see, the low altitudes. It exploits a TIN network method explained in figure 3.4. The algorithm was implemented using the ArcGIS software to save time. Nevertheless, a similar procedure can directly be implemented in any climate models. In Appendix A, a list of all procedures implemented in ArcGIS can be found.

Figure 3.5 illustrates the six steps performed to obtain the final DEM. Firstly, we need to isolate summits or peaks in the study area. To achieve this, two steps are necessary: (a) the values of the pixels in the input DEM are replaced by the maximum altitude inside a circle with a specific radius equal to the user-defined output DEM resolution (in our case 20 or 10 km). After that, (b) the difference between the input DEM and the local maximum found in (a) allows us to isolate the summits. These peaks are the nodes used in (c) the TIN construction. The latter is then (d) rasterised and finally (e) an extraction in this raster is done at each pixel of the output DEM. It should be noted that this procedure can be iterative and an extra step (f) can isolate a surplus of summits by deducting the TIN raster with the former input DEM. In this way, we can add the points above the TIN raster into the set of peaks and restart the TIN construction at step (c) with the improved peaks set. In our study, two iterative operations were performed.

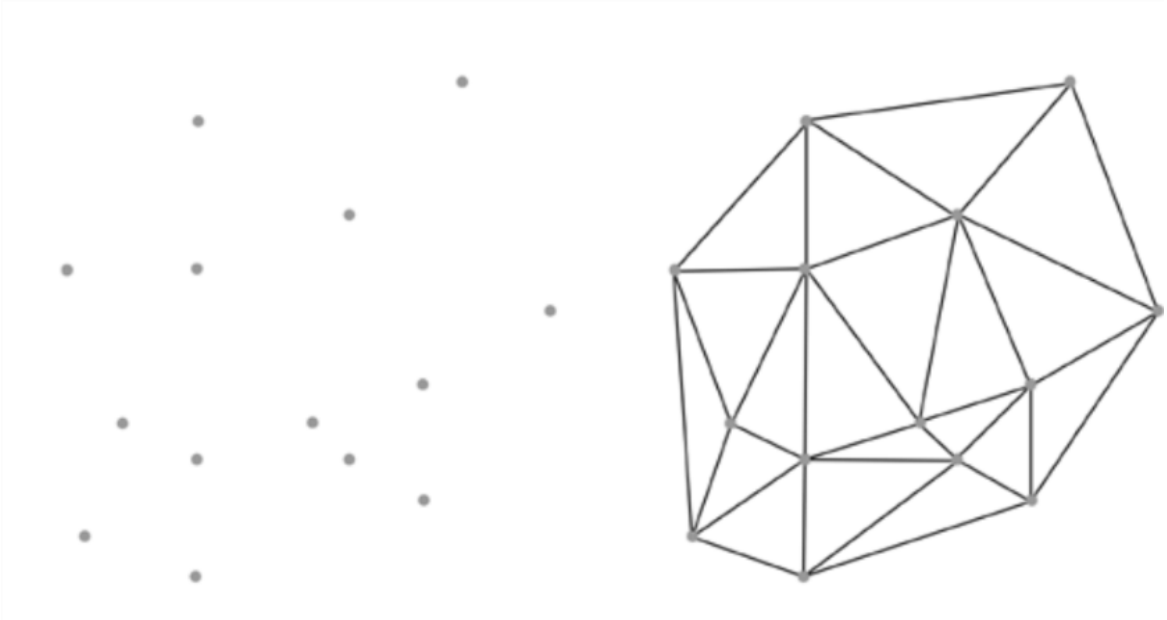

Figure 3.4 TINs are constructed from a series of irregularly nodes (left scheme) that are in some way meaningful for the surface (i.e., peaks, valleys, places where slope changes abruptly, etc.). Each point is connected to its nearest neighbours using a technique called Delaunay triangulation (right scheme). Adapted from https://www.e-education.psu.edu/geog486/l6.html.

(iii) Thalwegs and crests method (TC method)

The two previous methodologies are focused on enhancing high altitudes, e.g. reproducing the blocking effect. However, the representation of valleys and plains plays a primal role in climate modelling. This enables a more consistent picture of temperatures, precipitation, wind fields and other climatic variables. The aim of this third additional method is therefore to satisfy this need while maintaining as many peaks and mountain ridge as possible. This method therefore keeps both high frequencies (low altitudes points with valleys and high altitudes point with crests), and thus enhances the high relief amplitude. Consequently, the slope between pixels will increase. Once again, we used ArcGIS to implement the algorithms and save time. Nevertheless, a similar procedure could be directly implemented in any climate models. In Appendix B, a list of all GIS procedures implemented in ArcGIS can be found.

The initial idea of this method consists in identifying a series of watersheds and thalwegs (line of maximum area drained) in our study area using a series of hydrological procedures.

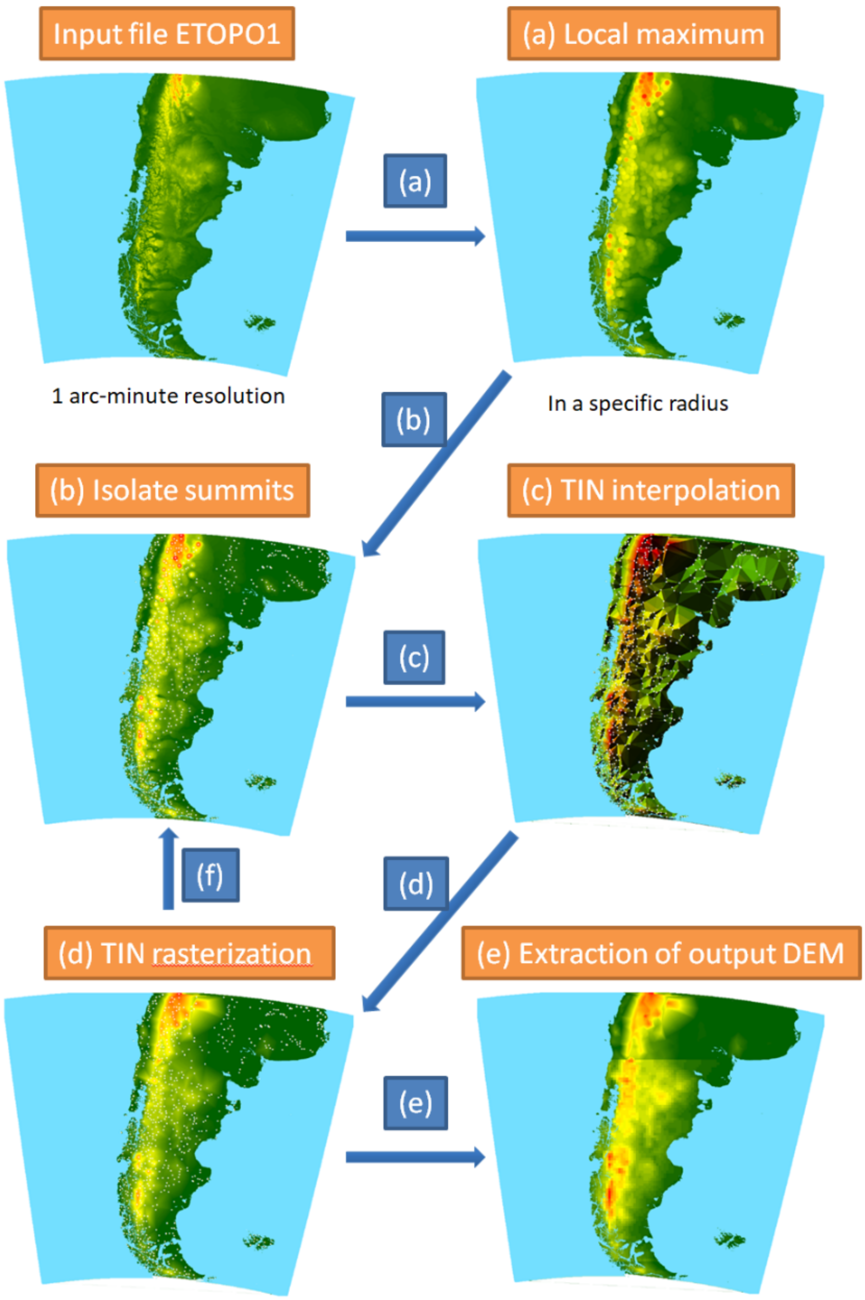

Figure 3.5 Representation of the six steps performed in ARCGis within the EM method. The blue rectangles and arrows represent the six steps and the orange rectangles represent the result of the six steps. (a) The values of the pixels in the input DEM are replaced by the maximum altitude inside a circle with a specific radius equal to the user-defined output DEM resolution (in our case 20 or 10 km). (b) Difference between the input DEM and the local maximum found in (a) allow us to isolate the summits. (c) TIN construction where the nodes are the peaks retrieved in (b). (d) Rasterisation of the TIN construction. (e) Extraction of this raster retrieved in (d) at each pixel of the output DEM. (f) Additional step to isolate a surplus of summits by deducting the TIN raster retrieved in (d) with the former input DEM.

Initially, as Wu et al. (2008) have noted, we consider the presence of sinks. A DEM sink occurs when all neighbouring cells are higher than the central cell, which has no down-slope flow path to a neighbour cell. Sinks could be the result of real components of the terrain, but also of input errors. They lead to errors in the computation of flow direction and of flow accumulation. The sinks are therefore commonly removed prior to DEM processing for a more consistent watershed identification. Then, we identify a series of thalwegs thanks to a reclassification of the flow accumulation raster with values superior to 50 pixels, value that we judged significant for a thalwegs identification. This reclassification combined to the flow direction computation allows us to identify a series of watersheds.

Figure 3.6 shows a portion of the area with the resulting watersheds and thalwegs. Note that watershed borders correspond to crests.

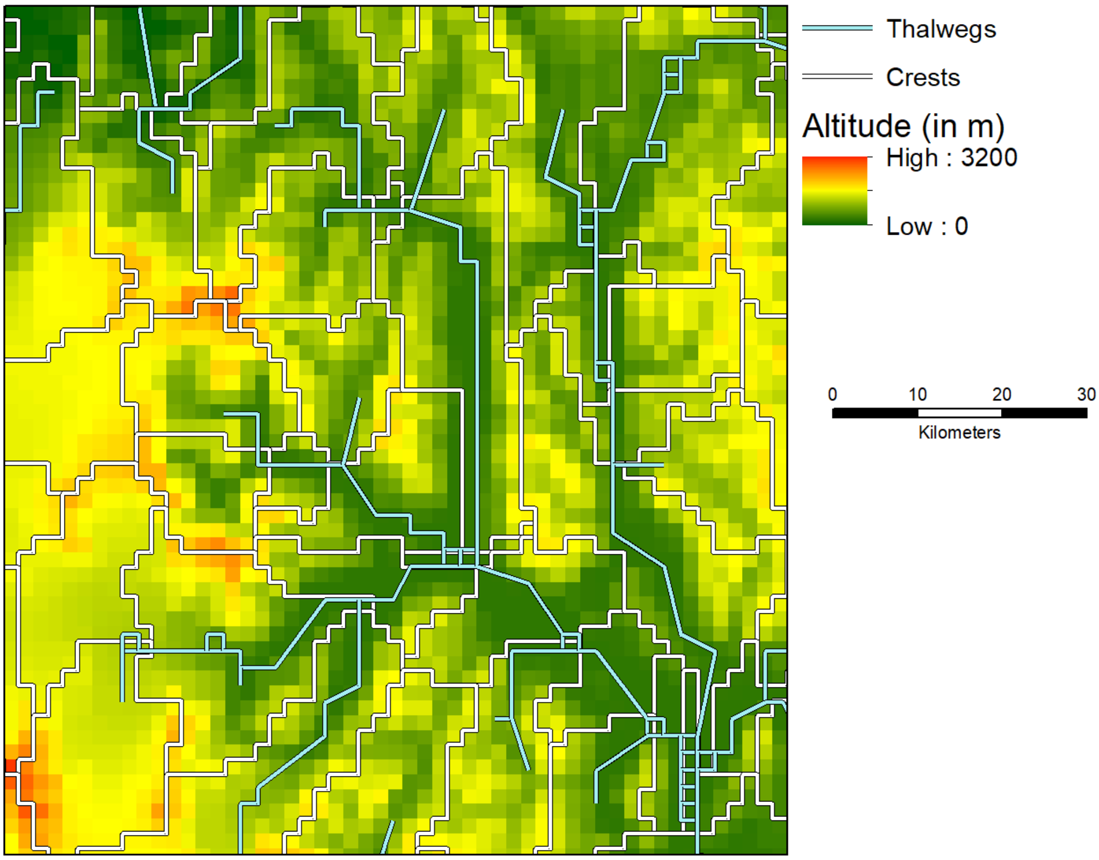

Figure 3.6 Sample region of our domain showing thalwegs and crests retrieved using ArcGIS within the TC method.

Subsequently, the altitude of each pixel is calculated according to its proximity to the closest crest and the closest thalweg. Four variables per pixel are needed to calculate its altitude. Firstly, two cost values are attributed to all pixels on the input high-resolution DEM depending on their distance to (i) the closest thalweg and (ii) the closest crest. It should be noted that the cost distances are not calculated thanks to a classic euclidean way but thanks to the direction of the flow. Figure 3.7 and figure 3.8 show the thalweg and crest cost distance raster respectively. In addition to the cost distances, we attribute to all pixels the altitude value of (iii) the closest crest and (iv) the closest thalweg. Then, the two cost distance rasters are needed to calculate if each pixel is closer to a crest or to a thalweg. In the first case, the altitude of the pixel will be the altitude of the crest, in the second case the altitude of the thalweg. Both are retrieved from the (iii) and (iv) rasters. Figure 3.9 shows the altitude attribution of a subset of the study area depending on their proximity with crest or thalweg.

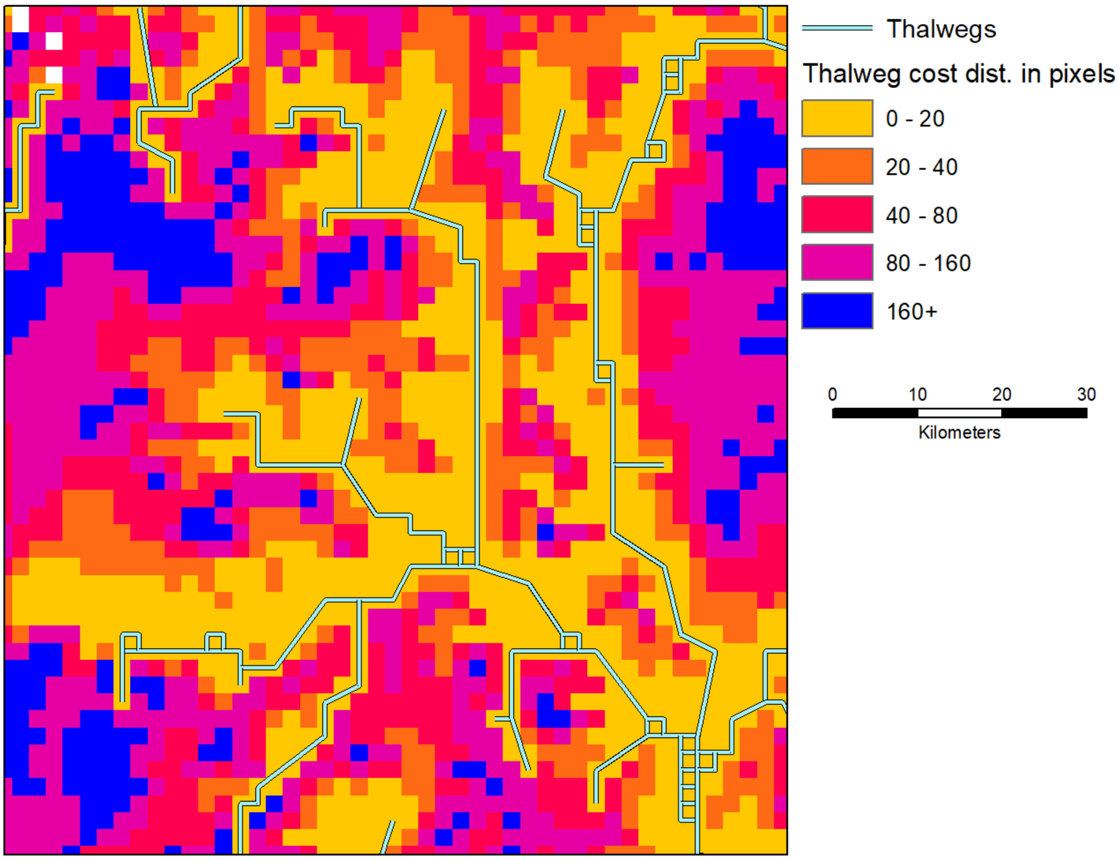

Figure 3.7 Sample region of our domain showing the output result of the cost distance analysis computed by ArcGIS to the closest crest (represented by blue lines) within the TC method.

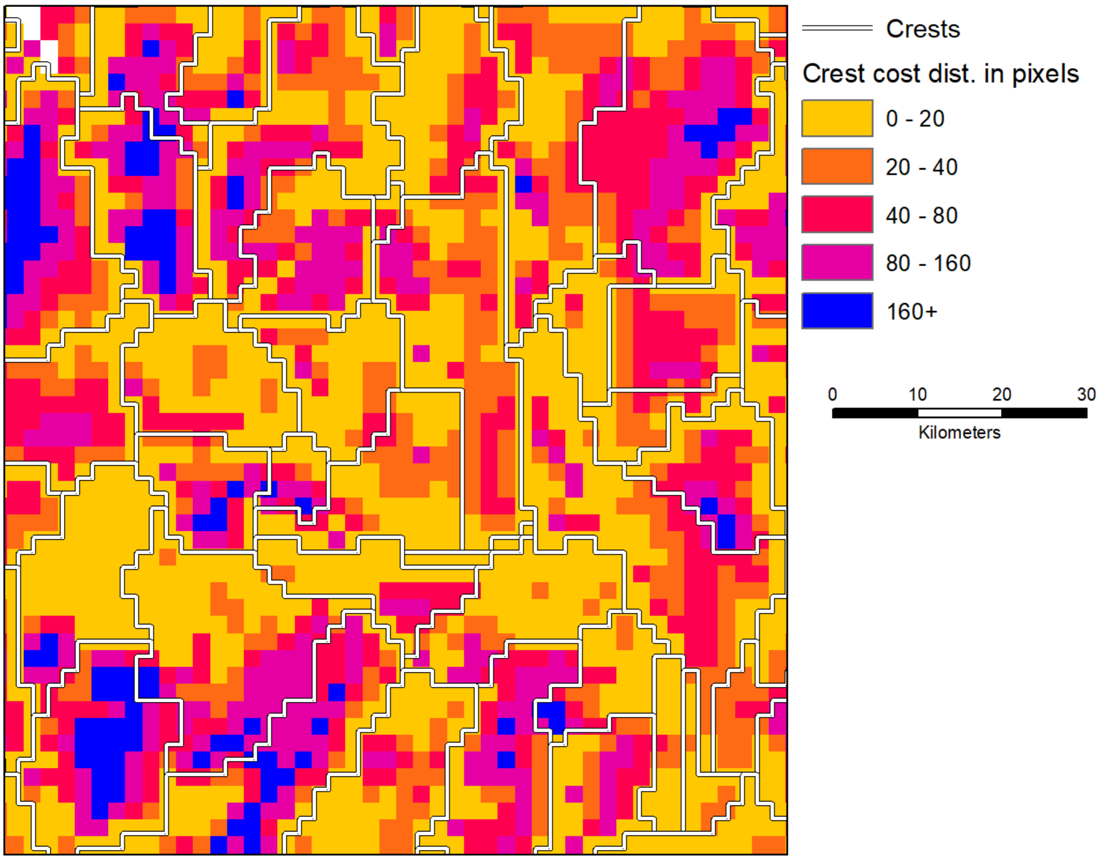

Figure 3.8 Sample region of our domain showing the output result of the cost distance analysis computed by ArcGIS to the closest crest (represented by white lines) within the TC method.

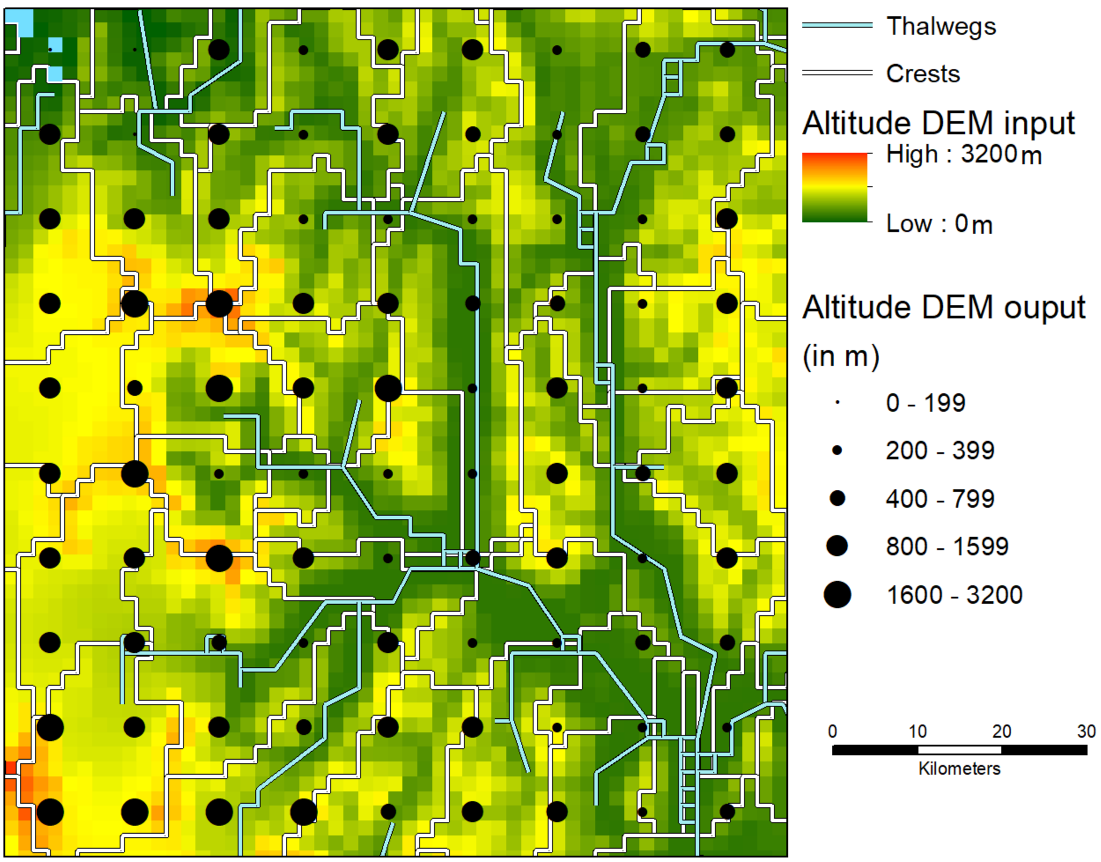

Figure 3.9 Sample region in our domain showing altitude attribution of the low-resolution grid from the high-resolution grid (ETOPO1) using the thalwegs and crests method within the TC method. The pixels altitude of the low-resolution grid (represented by the black dots) are retrieved from a friction cost analysis between each dot and the DEM input altitude of the closest thalweg or crest (represented by, respectively, the blue and white lines).

It should be noted that our method is experimental and can be improved in different ways. For example, a crucial step in this method is the identification of the thalwegs in our region. As explained earlier, this identification is performed by a reclassification of the flow accumulation raster. The threshold of this reclassification, fixed at 50 pixels in our study, needs to be computed multiple times to find the most appropriate value which takes into account a relevant number of thalwegs. Instead of selecting one value, we could retrieve several DEM from this method using several different thresholds. Taking another example, we could weight the altitude according to the distance. If a pixel is closer to a thalweg or a crest, then its altitude value is closer to the thalweg or the crest in question.

3.5.2 Influence, pros and cons

Figure 3.10 shows the different output low-resolution DEM obtained using the four DEM generalization.

In this section, we discuss the difference between the four DEMs obtained. A generalization is considered to be accurate if its result shows spatial altitude frequencies close to the former high-resolution DEM. We chose to illustrate these frequencies in two graphical ways: a series of transects and a histogram of relative and cumulated frequencies. We have deliberately chosen not to illustrate this DEM generalization comparison with maps because it would require an interpolation of the low-resolution DEM at the former high-resolution input DEM. As a consequence, the accuracy of the resulting interpolated DEM would depend on the interpolation used and not only on our former four generalizations.

First, a transect consists of a spatial representation, along a linear path and following the vertical dimension, aimed at emphasising a superposition between different layers. We have chosen four different transects (figure 3.11) to observe different specific orographic features in our study area. Transect A crosses the region in its highest peak. Concerning transect B, its aim is to understand which generalization can better perform an orographic abrupt break, a typical feature of our region. Transect C crosses the region between two high peaks and finally, transect D crosses the region in flatter areas.

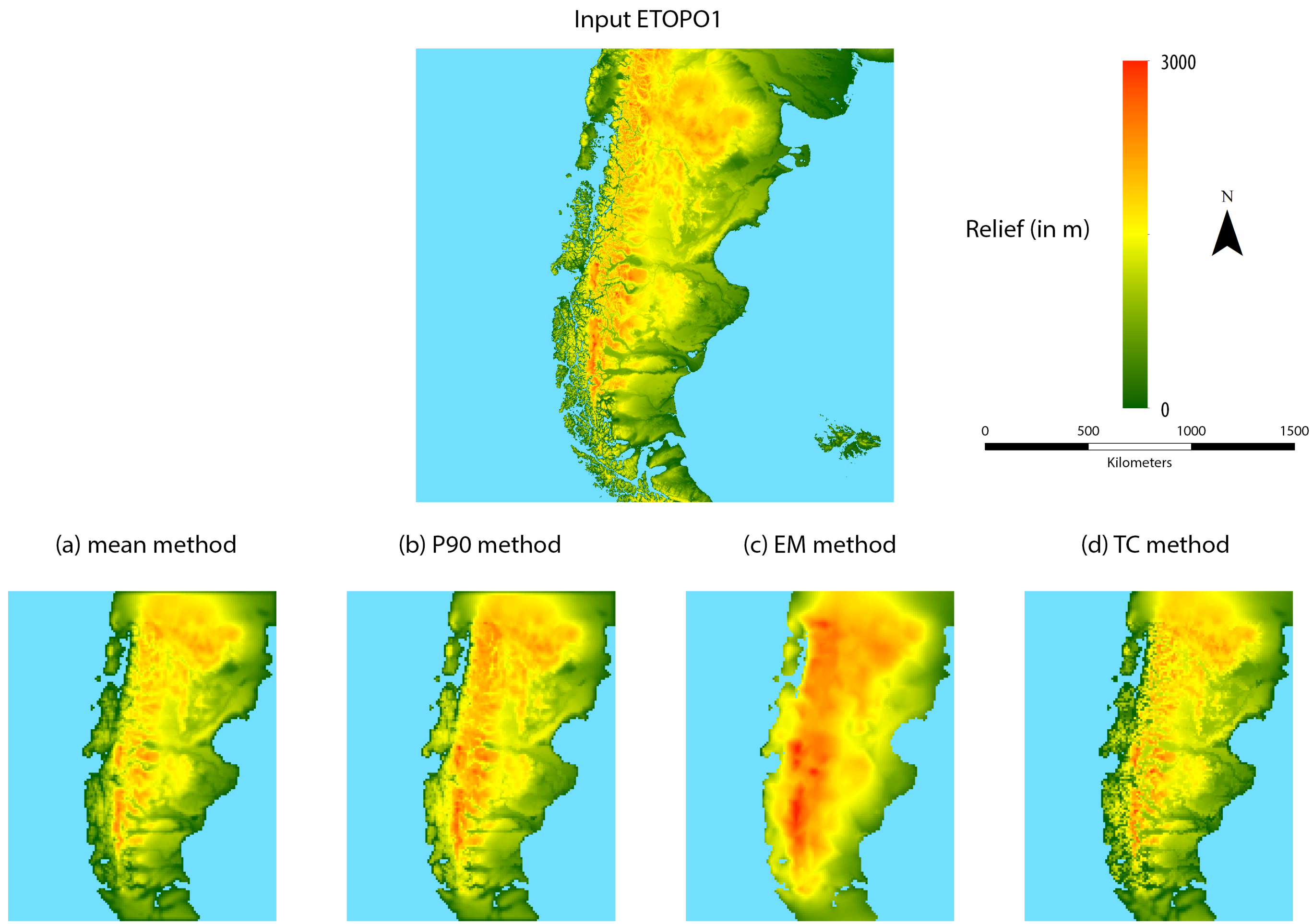

Figure 3.10 Final results of the four DEM generalization methods. From the same input DEM ETOPO1 at a 1 arc-minute resolution, we obtained four different output DEM at a coarser 10 km resolution, using four different DEM generalization methods. The methods performed are (a) the mean method, (b) the percentile 90 method, (c) the envelope maximum method, and (d) the thalweg and crests method.

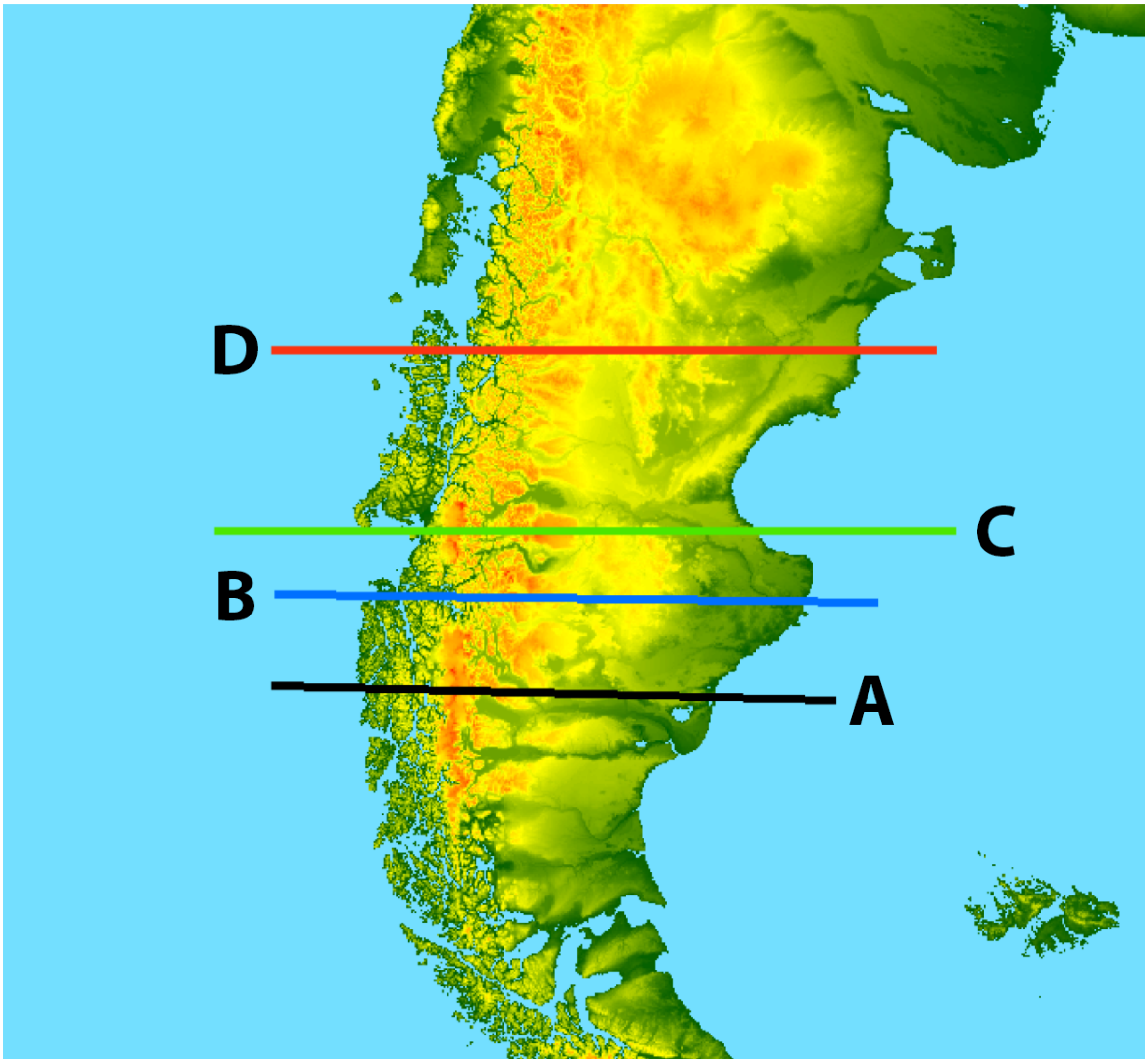

Figure 3.11 Four profiles of the vertical surface elevation. The aim is to show the performances of each DEM generalization method with respect to the original DEM.

- The transect A (3.12) shows that only the envelope method can reproduce the highest peak of the area because its algorithm primarily takes into account major peaks to interpolate a surface elevation. However, this method deeply smoothes valleys and rises plains in all transects. The mean method is the opposite, with a smoothing of the peaks and a more consistent representation of the valleys. The thalwegs and crests and, in some way, the percentile 90 methods seem to be a good tradeoff, where P90 performs slightly more consistently in high altitudes while the thalweg methods is clearly more consistent in valleys.

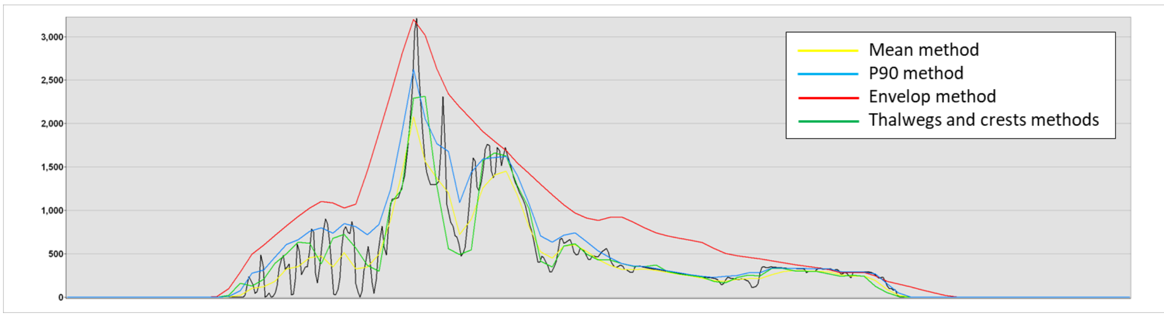

Figure 3.12 Surface elevation profile A

- As expected, transect B (3.13) illustrates a very poor representation of the abrupt break by the envelope method. The area is situated between two peaks which is difficult for this method to represent. Apart from that, the three other methods are similar, with P90 again slightly more consistent with peaks but less with valleys.

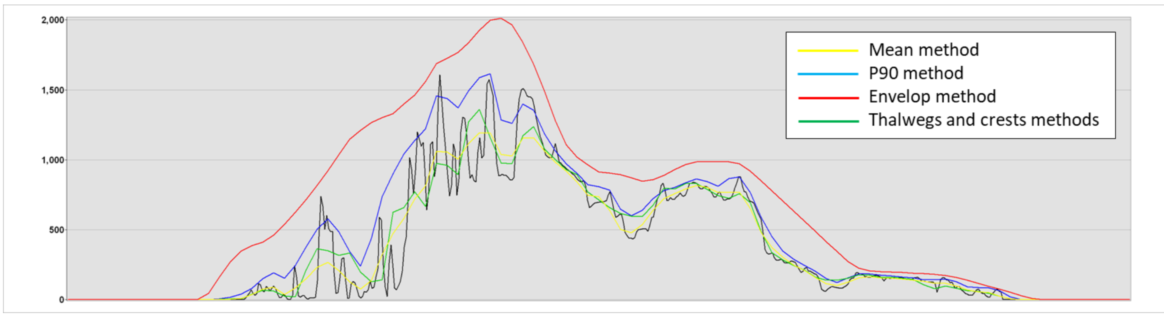

Figure 3.13 Surface elevation profile B

- Transect C (figure 3.14) shows that only the mean and TC methods are able to reproduce the surface elevation between two peaks, where TC seems, again, to be more similar to the original DEM.

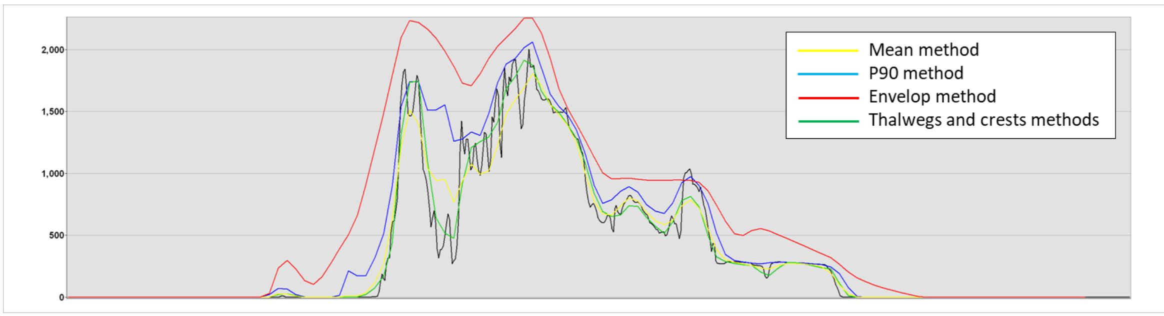

Figure 3.14 Surface elevation profile C

- Lastly, transect D (figure 3.15) confirms our former ascertainments with valleys and plains altitudes overestimation by envelope and, in some way P90, and correct representation by mean and TC method.

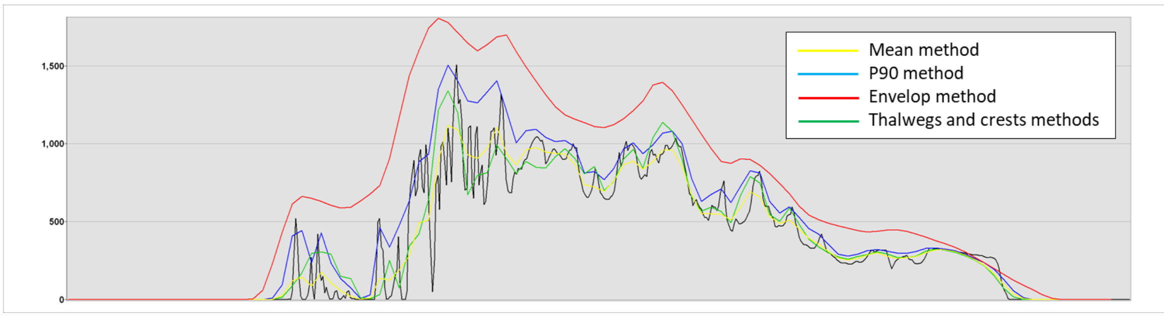

Figure 3.15 Surface elevation profile D

For our second graphical method, we display relative cumulated frequency histograms of altitude values over the whole area of interest and for the four methods in figure 3.16. The closer the frequency curve of a method is to the curve of the original surface elevation the more consistent the method could be considered. The mean and TC methods are therefore the most consistent because their frequency curve is nearly similar to the one of our input DEM. Concerning the P90 and more the envelope method, they fail to reproduce the same distribution, especially between 500 to 1500 m. It should be highlighted that in our case, we are mainly looking for a generalization method which can reproduce the blocking effect of the Andes, e.g. really high altitudes (see the maximum altitude represented by vertical lines in figure 3.16). From this point of view, the EM method seems to be the more adequate followed by the TC and P90 methods.

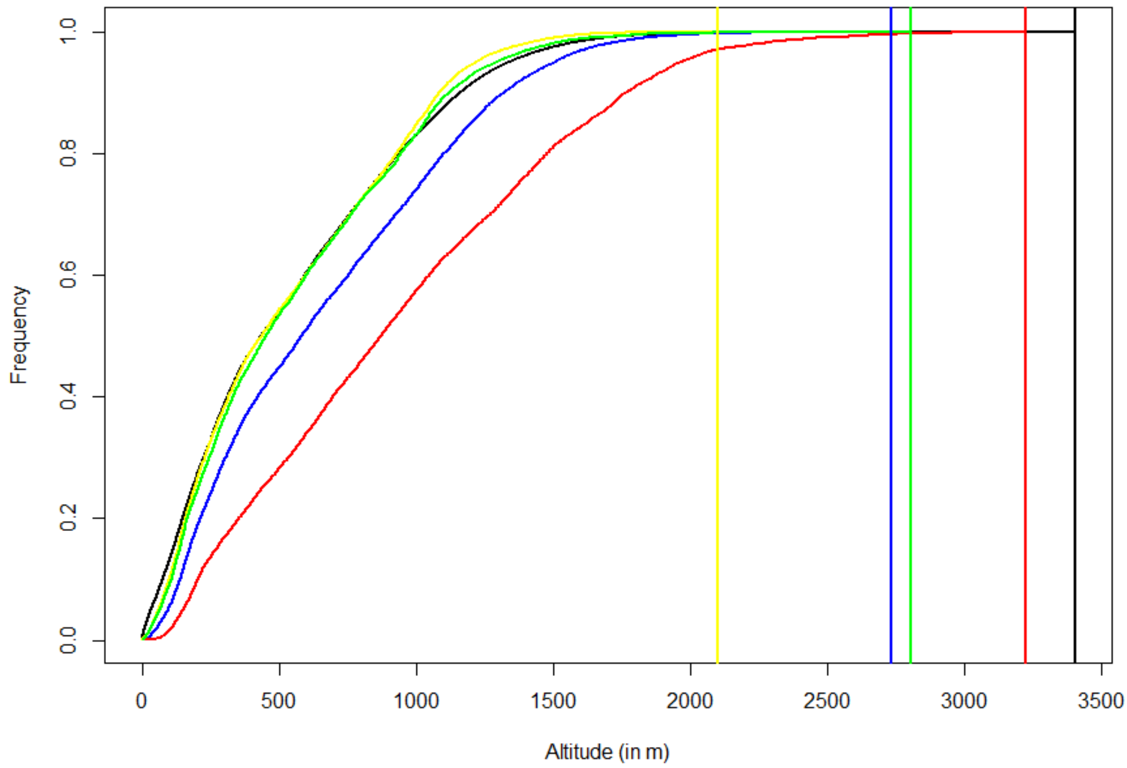

Figure 3.16 Cumulative frequencies histogram of altitude with the four DEM generalization methods. The black curve represents the histogram of the original input DEM ETOPO1, the yellow one represents the mean method, the blue one represents the percentile 90 method, the red one represents the envelope maximum method and the green one represents the thalwegs and crests methods. The vertical lines represents the altitude of the uppermost pixel. The closer the curve of a method is to the curve of the original surface elevation the more consistent the method could be considered.

3.6 Conclusion

This chapter reflects the diversity of DEM generalization methods, a crucial step in surface elevation modelling that is too often neglected in climate models. We tried to develop three additional methods to the standard mean box method used in nearly all RCMs or GCMs. Our two comparative analyses show us corroborating results. The TC method followed by the mean method are the closest to the original input DEM. However, in our study case, methods like P90 or EM could bring concrete added value with a more consistent representation of the blocking effect. Lastly, it should be highlighted that, even if the TC method produces impressive qualities in our graphical and statistical analysis, the latter presents a highly irregular surface with valley pixels close to peak pixels and very steep slopes. There is therefore a risk to get more instability produced by a climate model.

The next logical step is to use these three different methods in our regional climate model to observe the sensitivity of MAR to those inputs and their influence on computed climatic variables.

Chapter 4

Influence of DEM generalization in MAR

To evaluate the influence of DEM generalization on climatic variables, a reference run and three DEM generalization sensitivity experiments are performed by the version 3.9 of the Regional Climate Model MAR on our study area, Patagonia. The aim of the first simulation consists in evaluating the performance of the model with the Climate Research Unit (CRU) gridded climate datasets. The second step includes a series of sensitivity experiments. Each experiment includes a change in the DEM generalization method, addressed in the previous chapter, to assess the impacts of the surface elevation generalization on MAR outputs. In other words, we call "DEM generalization sensitivity experiments" the experiments that evaluate the sensitivity of MAR to the DEM generalization inputs.

The focus of our research is on warm and dry air masses resulting from Foehn winds situated on the east side of the Andes mountains. The objective is thus to observe the performance of the model in reproducing these effects and assess if our generalization experiments can improve the climatic model outputs.

The MAR inputs, outputs as well as the set-up and forcings used in simulations and the validation are discussed in the following two sections. The third section addresses the results of the reference run and the DEM generalization sensitivity experiments.

4.1 The Regional Climate Model MAR

The Modèle Atmosphérique Régional (MAR), developed by, inter alia, H. Gallée from the Laboratoire de Glaciologie et Géophysique de l'Environnement (LGGE) and X. Fettweis from the University of Liège (ULiège), is used throughout our study. An RCM has been selected here since the spatial resolutions of GCMs are too coarse to accurately simulate events like Foehn events in Patagonia (Seluchi et al. 2003 ; Klink 1995). The MAR model consists of a three-dimensional meso-scale primitive equation atmospheric model that can predict the evolution of a defined and restrained coupled land-atmosphere domain (Gallée and Schayes 1994; Fettweis et al. 2005). The atmospheric part of MAR is fully described in Gallée and Schayes (1994) and Gallée et al. (1995). The RCM is coupled to the 1-D SISVAT (Soil Ice Snow Vegetation Atmosphere Transfer) module described in De Ridder and Gallée (1998). This involves three different sub-modules; (1) the soil and vegetation sub-module, (2) the snow sub-module and (3) the ice sub-module (Kittel et al. 2018). They simulate energy and mass fluxes between the surface and the atmosphere. The model was formerly developed to simulate katabatic winds in Gallée and Schayes (1994) and its ability to simulate these winds has been extensively agreed (Barthélemy et al. 2012 ; Mathiot et al. 2010; Gallée and Pettré 1998). Following these previous works, The MAR model seems therefore a perfect candidate to simulate Foehn events which, although they are not similar, have some similarities with katabatic winds.

The MAR atmosphere and surface boundaries are forced every six hours by the ERA-Interim reanalysis developed by ECMWF at a 0.75°x 0.75° spatial resolution. The methods and satellite observations assimilated into ERA-Interim reanalysis are described in Dee et al. (2011).

The MAR pre-processing treatments are produced by an independent tool called NESTOR (NESTing Organization for the preparation of meteorological and surface fields in Regional models). The aim of the latter is to interpolate the climatic variables from ERA-Interim reanalysis and to initialise the MAR domain. The generalization of the relief from the high resolution ETOPO1 raster to the low-resolution used by MAR occurs during this initialisation. We needed therefore to go inside the source code of NESTOR to replace its former DEM generalization method by the ones we have developed.

4.2 Validation and Climate Research Unit (CRU)

As discussed in Chapter 2, the Patagonian meteorological network is not considered sufficient to describe climate variability and verify climate models. For that reason, our study uses observational gridded climate datasets as an alternative approach, to verify climate models. Previous studies have shown the real benefit of this method to overcome the meteorological network limitation of our region of interest (Bianchi et al. 2016). Notwithstanding the knowledge of this limitation and the benefits of gridded climate datasets, few recent studies have chosen this validation method and have preferred in-situ measurements. It should be noted that other scholars have pointed out that the quality of observational gridded climate datasets in complex relief is, however, questionable (Solman et al. 2013).

Among all the gridded climate datasets available, we have decided to carry out our model validation exclusively with the Climate Research Unit (CRU) database. The CRU TS v.4.01 database at a resolution of 0.5° latitude produced at the University of East Anglia is used. The variables retained are the mean temperature and the precipitation, key components of the climatic variabilities of Foehn events. The development and verification of this database is documented in Harris et al. (2014).

4.3 Simulations using MAR

Simulations of MAR are used in two ways; (1) the evaluation of MAR and (2) three DEM generalization sensitivity experiments. They are discussed below and schematically represented on figure 4.1. The red or black rectangles on the following maps represent the lee sides of the mountains, where warm and dry air masses are expected. This will be our region of interest in the next analyses.

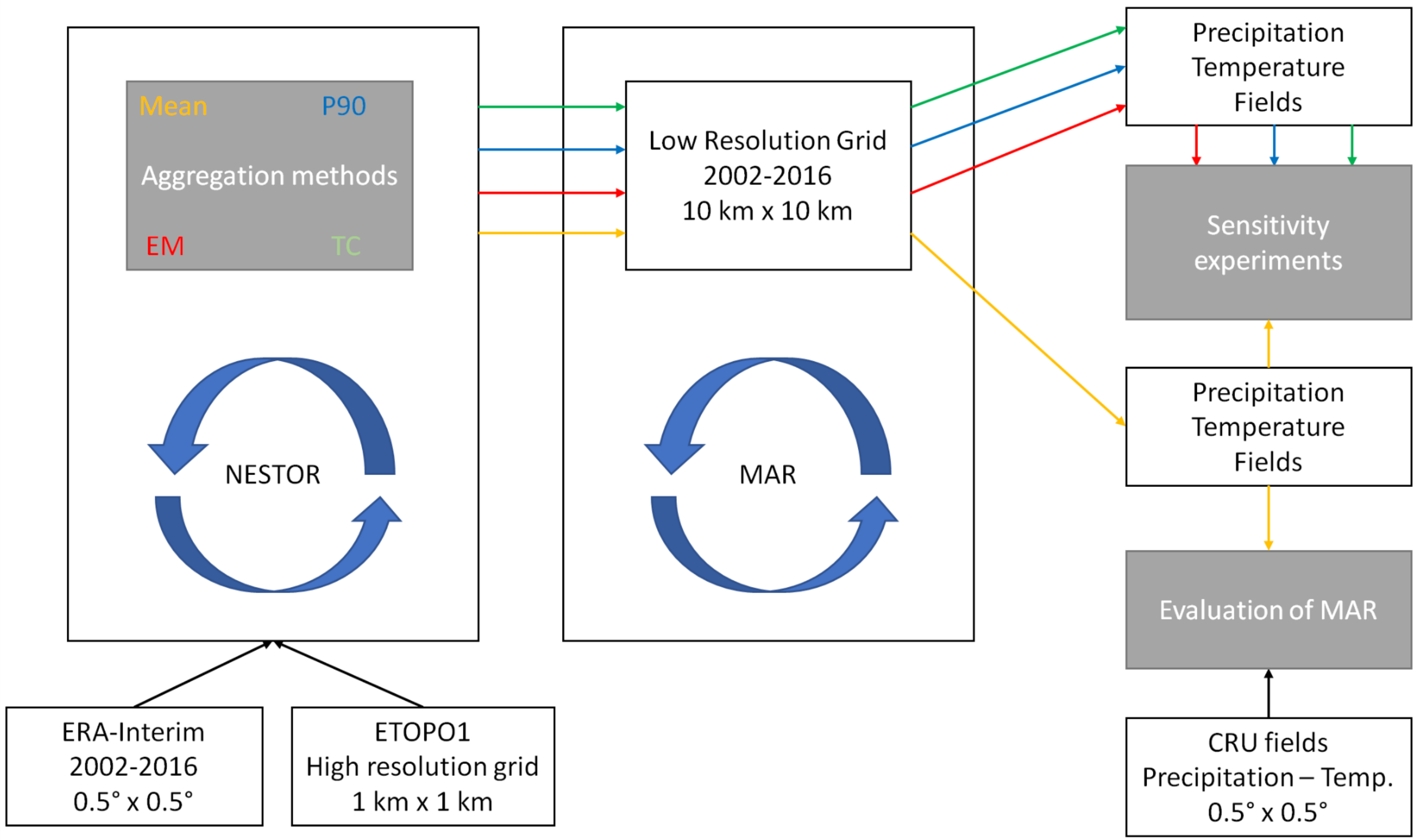

Figure 4.1 Summary of the methodology used in our research to perform the sensitivity experiments and the evaluation of the MAR. Mean = mean method (initial method), P90 = percentile 90 method, EM = envelope maximum method, TC = thalwegs and crests methods.

4.3.1 Evaluation of MAR

A first reference run of the region of interest performed by the latest version of the MAR, using the former generalization method (the mean method), is evaluated compared to the CRU grid during the period 2002-2016. Using a Fortran script, we performed a bilinear interpolation to compute the pixels value of the CRU grid from the MAR grid. No height correction has been applied in the interpolation procedure. That means we did not take into consideration the surface elevation difference between the interpolated MAR grid and the CRU grid, shown in figure 4.2, with values varying between +100 m and -100 m.

The aim of this simulation is to observe the performance of the model in predicting Foehn events and its meteorological consequences in our region. We therefore subtracted the MAR outputs (precipitation and mean temperature over the 2002-2016 period at two spatial resolutions; 20 and 10 km resolution) of the reference run interpolated on the CRU grid, from the CRU fields.

Temperature results

Figure 4.3 shows a general underestimation of -1°C to -2°C, and locally -3°C, by MAR compared to the climate datasets CRU in our region of interest. It is important to note that this underestimation is more pronounced on high altitude areas where CRU turns out to be less accurate (Solman et al. 2013). As a matter of fact, figure 4.4 illustrates that the higher the pixel altitude, the greater is its mean temperature bias. In the end, these results are similar to the commonly agreed underestimation of mean temperature discussed in our literature summary, Chapter 2.

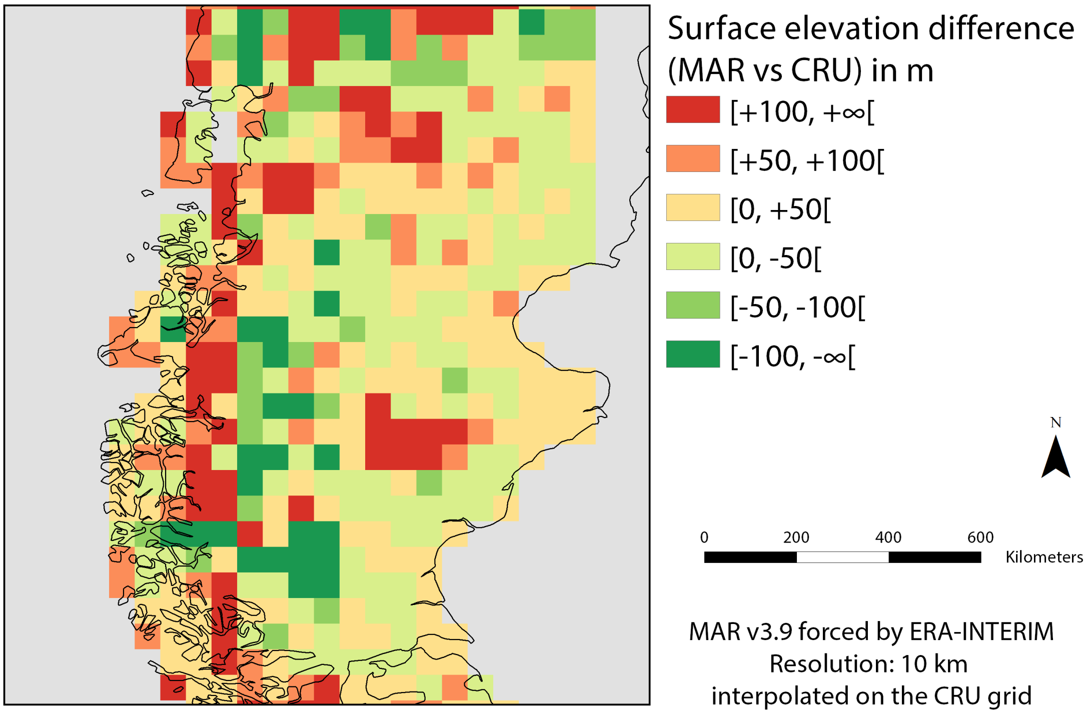

Figure 4.2 Surface elevation difference in Patagonia between the MAR surface elevation at 10 km spatial resolution interpolated on the CRU grid, and the CRU surface elevation at 0.5°spatial resolution. Red colours mean that the DEM retrieved by MAR is higher than the DEM used in CRU, whereas green colours mean that the DEM used in CRU is higher.

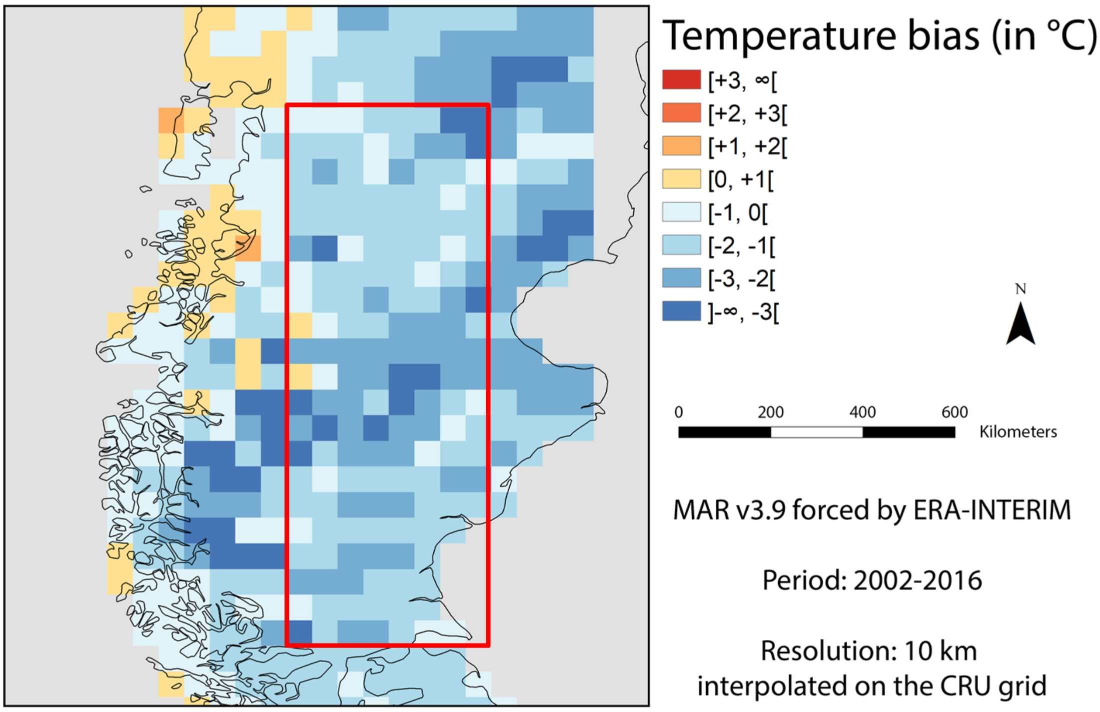

Figure 4.3 Bias of annual mean of 2 m temperature in °C using the MAR model over 2002-2016 compared to CRU in Patagonia. The red rectangle is our region of interest where a clear negative temperature bias can be observed.

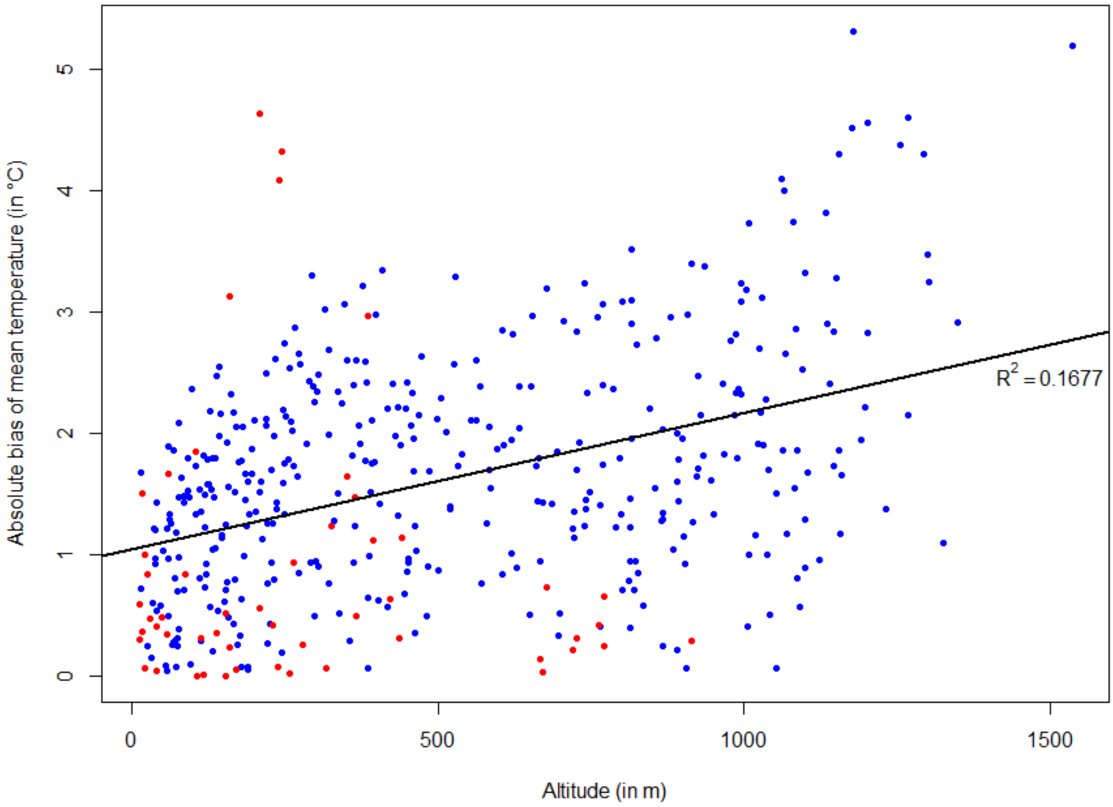

Figure 4.4 Each point represents the altitude (in meters) and the absolute bias of mean temperature (in °C) of a pixel of the CRU grid. Note that the altitude is derived from the MAR DEM model using the DEM generalization mean method interpolated on the CRU grid. Blue pixels represent the pixels of the area where the mean temperature bias is negative compared to CRU, whereas red ones represent the positive bias. The black line represents the linear regression (based on the least-squares method) of the two displayed variables with its respective residual standard error R^2. We can observe a slight (because R^2 is low) relation between the altitude and the absolute bias of the mean temperature of the pixels. The higher the pixel altitude, the greater is its negative mean temperature bias.

Precipitation results

Figure 4.5 shows a general overestimation of the total sum of precipitation by MAR compared to the climate datasets CRU. Generally, the total sum of precipitation simulated is up to +100 mm to +400 mm per year compared to CRU with some slightly underestimation to -50 mm in local regions mostly in the South. These results are also similar to the overestimation observed in our literature summary, Chapter 2. It should be noted that even though the absolute surplus of precipitation is large, it is still less significant than the relative surplus of precipitation displayed in figure 4.6.

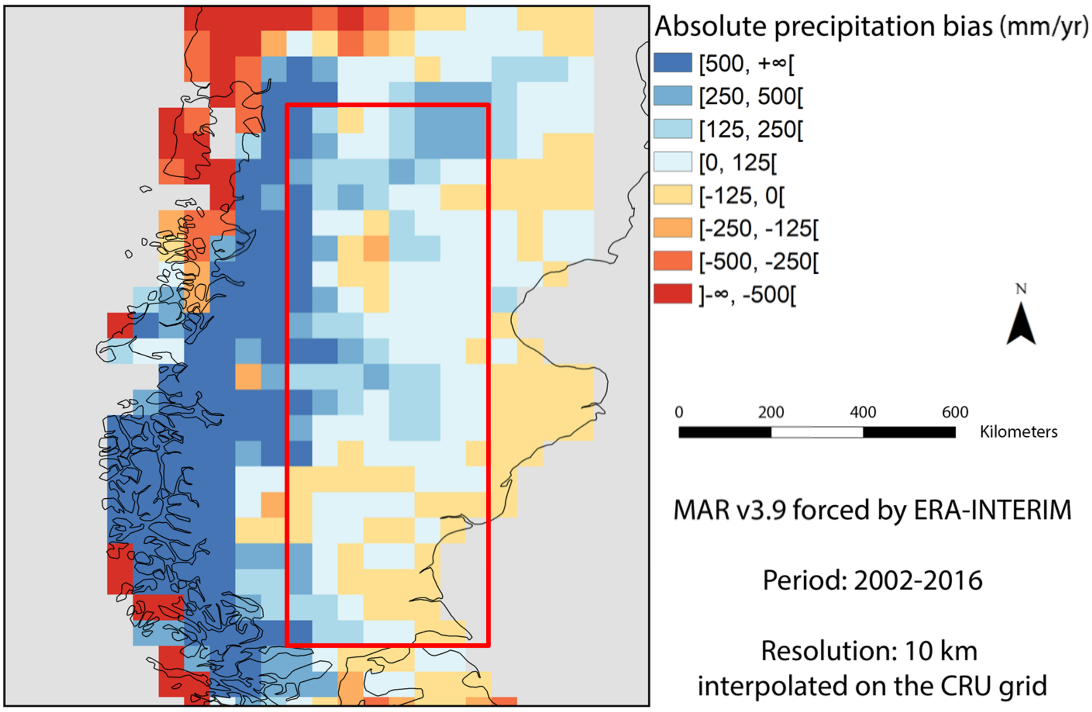

Figure 4.5 Bias of annual sum of precipitation (snow + rain) in mm/year using the MAR model over 2002-2016 compared to CRU in Patagonia. The red rectangle is the region of interest where a distinct positive precipitation bias can be observed.

Comparison between 20 and 10 km spatial resolution

The objective of this section is to observe if an enhancement of the spatial resolution from 20 km to 10 km can decrease the temperature and precipitation biases.

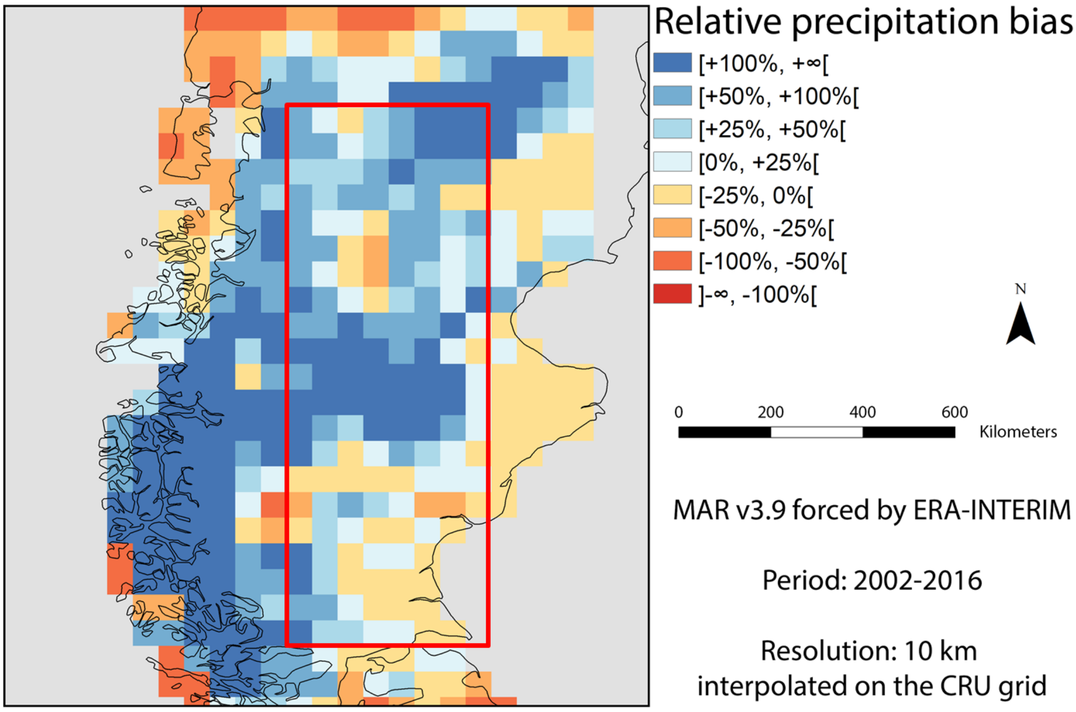

Figure 4.6 Bias of relative annual sum of precipitation (snow + rain) in °C using the MAR model over 2002-2016 in Patagonia. The red rectangle is the region of interest where a clear positive precipitation bias can be observed.

As we can see on figure 4.7 and figure 4.8, only the temperature variable is slightly closer to CRU with a 10 km spatial resolution, while there is no clear distinction between the precipitation bias of 20 km and 10 km resolution.

Consequently, a finer spatial resolution can improve the temperature output fields of our model compared to CRU. However, it cannot resolve the biases observed in the precipitation output fields.

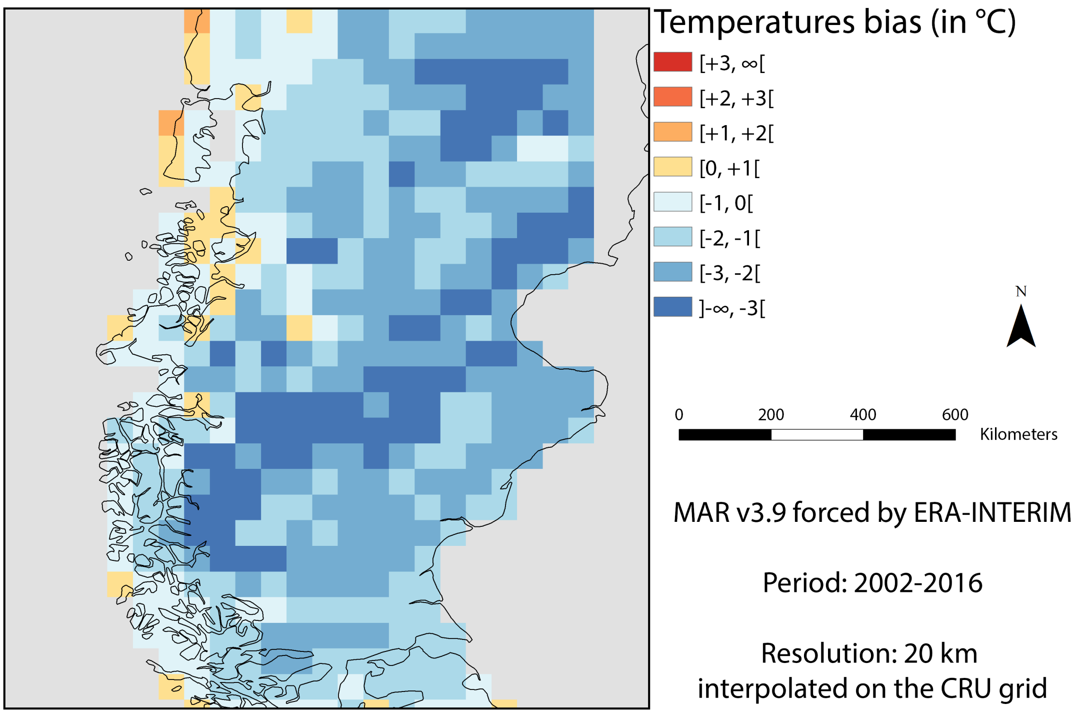

Figure 4.7 Bias of annual mean of 2 m temperature in °C using the MAR model with a 20 km spatial resolution over the 2002-2016 period compared to CRU.

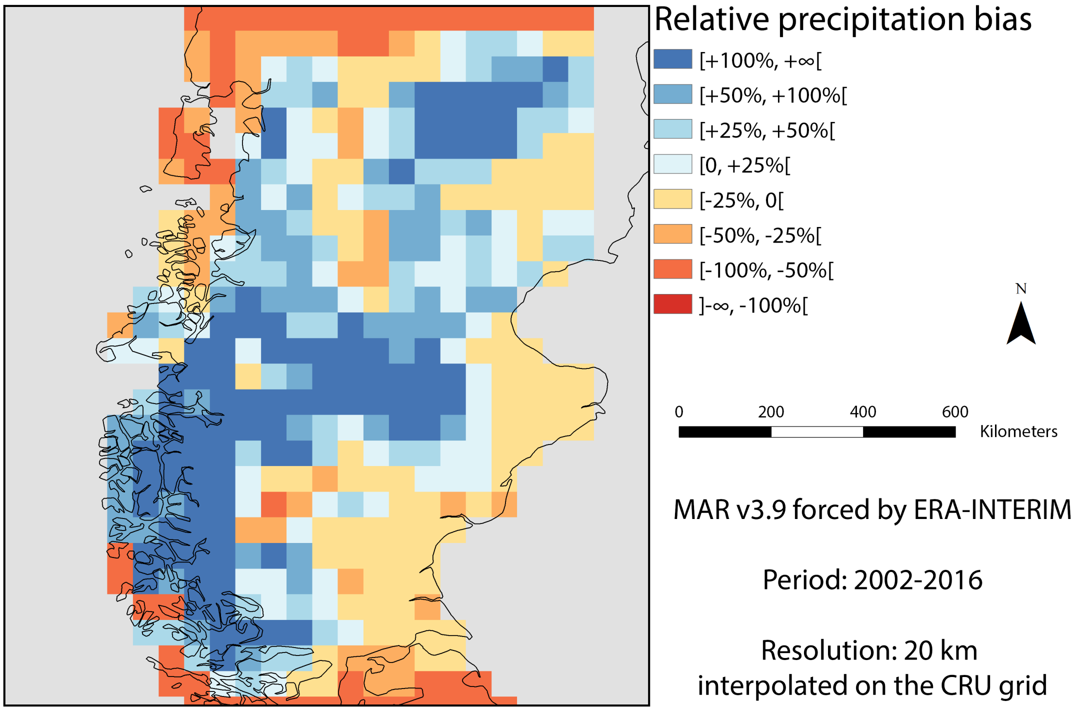

Figure 4.8 Bias of relative annual sum of precipitation (snow + rain) in mm/year using the MAR model with a 20 km spatial resolution over the 2002-2016 period compared to CRU.

4.3.2 DEM generalization sensitivity experiments

The second step consists of a series of DEM generalization sensitivity experiments to assess the influence of the surface elevation generalization on our model. Three simulations are performed by the MAR with three different surface elevations retrieved in the previous chapter over the 2002-2016 period. For each of the three simulations, the control parameter is the surface elevation model. The first is derived using the percentile 90 generalization method, the second with the envelope maximum method and the third with the thalwegs and crests method. Unlike the verification of the MAR, only the results at spatial resolution 10 km are discussed here because the 20 km resolution does not bring additional relevant information.

With these four simulations (the three experiments and the reference run using the mean method), an anomaly analysis using the difference between the output of each experiment and the reference run can be performed. Like the verification of the MAR, we focus on the spatial distribution of two variables; precipitation (rain + snow) and mean 2 m temperature.

Temperature anomaly

Figure 4.9 shows that, regardless of the method, DEM generalization has a huge impact on simulated temperature fields. MAR using (a) the P90 method produces a significant increase in temperature around 0.5°C to 0.75°C in a large part of our region of interest compared to the reference run, except in colder regions in the North. Outside the region of interest, temperature anomalies drop from -3°C to -4°C around the mountain range. With (b) the EM method, temperature anomalies drop significantly from -2°C to -3°C across all the region compared to the reference run. Only small south-easterly parts have positive annual temperature anomalies. Finally, (c) the TC method observations are significantly different from the other two. Temperature anomalies reach a general increase of +1°C to +2°C compared to the reference run. Moreover, this increase in temperature is constant outside the region of interest and only high local peaks show a decrease in temperature. Let us point out that the more pixelized appearance of this last method reflects the higher difference of altitudes between neighbouring pixels. This method therefore tries to reproduce more valleys and crests orographic features in the region.

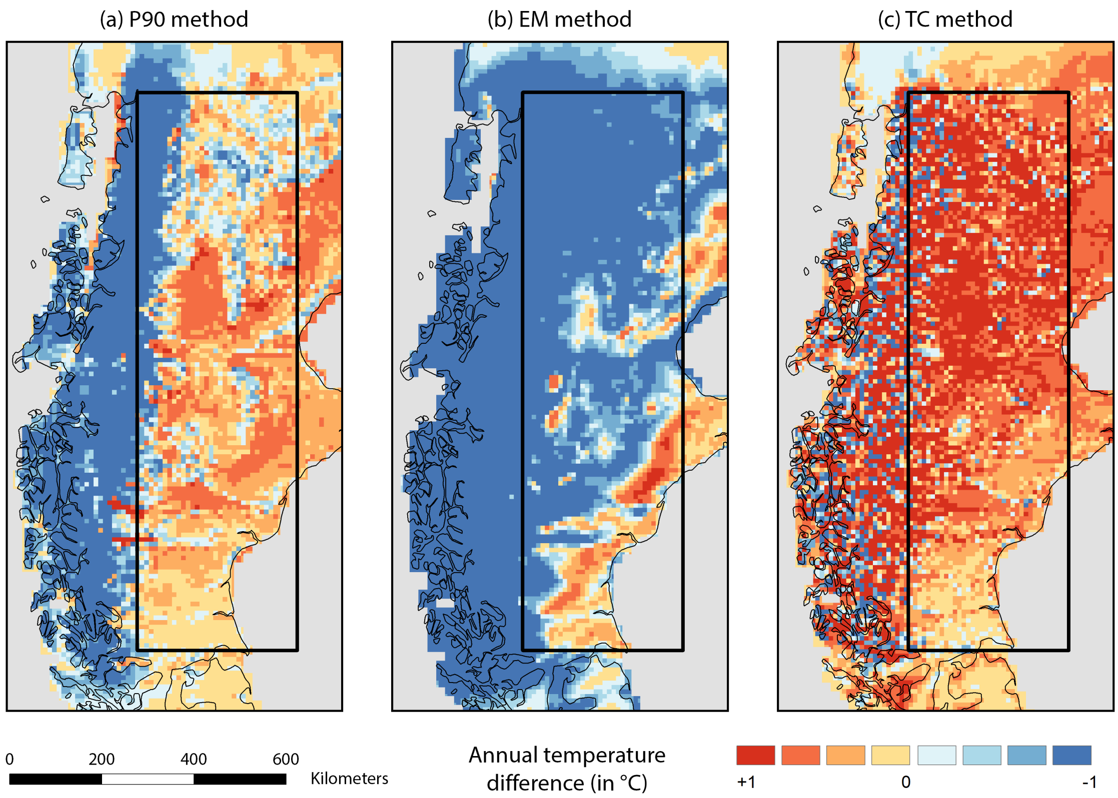

Figure 4.9 Anomaly in mean 2 m temperature in °C of (a) the percentile 90 method, (b) the envelope maximum method or (c) the thalwegs and crests method compared to the reference run. We use the v3.9 MAR model forced by ERA-INTERIM every six hours over the 2002-2016 period at a 10 km resolution. The black rectangle is the region of interest where two methods out of three (the (a) P90 and (c) TC methods) produce a significant increase in mean temperature. With (b) the EM method, temperature anomalies drop significantly.

Precipitation anomaly

DEM generalization also has a huge impact on simulated precipitation fields shown in figure 4.10. For example, the anomaly of annual precipitation of (a) the P90 method compared to the reference run induces a general decrease from -50 mm to -200 mm with high altitude areas in the centre of Patagonia reaching -500 mm. This decrease is similar but amplified with the anomaly of (b) the EM method. The general results of the latter are between -100 mm to -300 mm with local peaks reaching -650 mm. The results from the anomaly of (c) the TC method are distinctly different from the two previous methods. The anomaly shows a significant decrease in annual precipitation in the North with values reaching -50 mm to -100 mm and a slight increase of +50 mm in the south. Outside our region of interest, the results are also contrasting between an increase in precipitation for the (a) P90 and (b) EM methods and a decrease of precipitation for (c) the TC method.

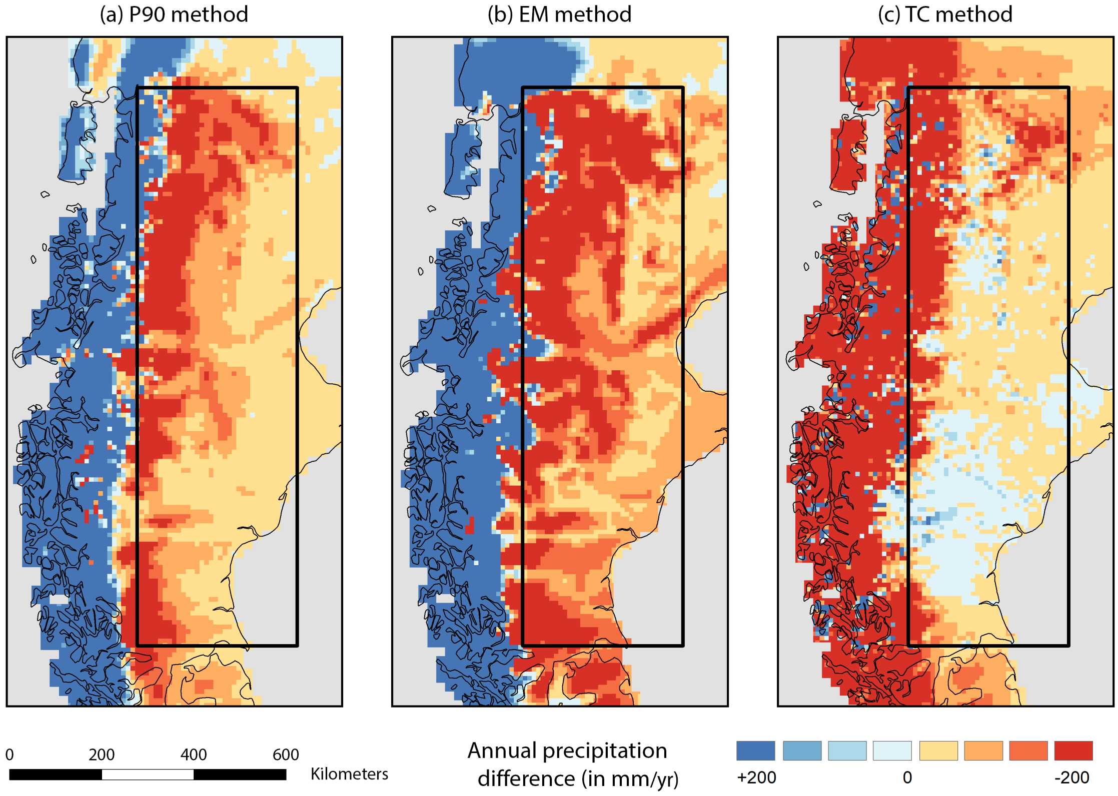

Figure 4.10 Anomaly in annual precipitation in millimetres per year of (a) the percentile 90 method, (b) the envelope maximum method or (c) the thalwegs and crests method compared to the reference run. We use the v3.9 MAR model forced by ERA-INTERIM over the 2002-2016 period at a 10 km resolution. The black rectangle is the region of interest where two methods out of three (the (a) P90 and (b) EM methods) produce a general decrease in precipitation. With (c) the TC method, precipitation decrease in the North and slightly increase in the South.

4.4 Results summary and discussions

Firstly, as expected, our evaluation of our RCM MAR shows an underestimation of annual mean temperatures and an overestimation of annual precipitation compared to CRU in our region of interest. As described in Chapter 3, this can be explained by the fact that the mean generalization method does not fully reproduce the mountain range, a key component to represent the blocking effect. The warm and dry air masses resulting from Foehn winds is therefore not well reproduced and lower temperature and higher precipitation can be observed on the east of the mountains compared to the CRU fields.

On the other hand, the DEM generalization sensitivity experiments were supposed to give us an insight on the surface elevation generalization capability to better reproduce the mountain range and, as a consequence, the warm and dry air masses. Results partially confirm this hypothesis with an increase in temperature for two out of three DEM generalization methods, but a negative anomaly in the EM method. The latter attributes altitudes significantly higher than the DEM input ETOPO1 used across all region and the temperatures are therefore mistakenly reduced. In terms of precipitation, only the P90 and EM methods induce a significant decrease in precipitation in the region of interest. The results are more contrasted for the TC method where precipitation decrease or increase depending on the areas. This could be related to the fact that our last method better represent the valleys at the expense of a perfect homogenisation of the mountain range. The air masses can therefore cross this irregular range and produce more precipitation. Finally, an increase in the instability expressed in Chapter 3 can also affect the precipitation modelling.

Chapter 5

Conclusion

5.1 Research context

Current RCMs and GCMs have always struggled to model Foehn effects in Patagonia. Studies carried out in the region emphasise that an inaccurate orographic representation is responsible for these precipitation-related modelling deficiencies. The most common technique to resolve this flaw is to improve the spatial horizontal resolution of the model to retrieve a finer and more complex surface elevation to the detriment of computation time and/or surface area coverage.

Instead of increasing the spatial resolution, this master thesis tackles the problem from a different angle by addressing DEM generalization. The aim of our study is twofold. The first objective is to assess different preselected DEM generalization methods and evaluate their ability to aggregate a complex orographic high-resolution DEM to a low-resolution DEM in our region. The second objective is to understand how the DEM generalization influences climate models and whether they can help us better model the Patagonian climate.

We work on the hypothesis that a better choice of DEM generalization method will allow us to better represent the mountain range in Patagonia. The cold air masses coming from the ocean would be therefore blocked by this range and hot and dry air masses, associated to the rain shadow effect, would be observed on the other side of the Andes. This would imply an increase in mean temperature and a decrease in precipitation over the eastern part of Patagonia.

5.2 Methodology

We developed three additional DEM generalization methods to the standard mean box method used in most RCMs and GCMs.

1. The percentile 90 (P90) method, which consists of a box method using the percentile 90 as statistical parameter.
2. The envelope maximum (EM) method, which identifies a maximum number of summits before performing a TIN network.
3. The thalwegs and crests (TC) methods, which derives the altitude of the low-resolution grid from an identification of thalwegs and crests in the region.

Firstly, we used two visual methods to compare the four DEM obtained, a series of transects and a histogram of frequencies.

Secondly, we evaluated their influence on climatic variables in Patagonia, using a reference run and three DEM generalization sensitivity experiments performed by MAR over the 2002-2016 period at a resolution of 10 km. The aim of the first simulation is to verify the standard performance of the model with the CRU gridded climate datasets. This part includes a comparison between the results at 10 km and 20 km spatial resolution to evaluate the influence of spatial resolution on the model. The second step involves a series of sensitivity experiments, to assess the influences of the DEM generalization methods on our model.

5.3 Results

DEM generalization analysis

The use of transects and the histogram of frequencies show corroborating results. The orographic features of the TC method followed by the mean method are the closest to the original input DEM. However, the other two methods, P90 and EM, bring concrete added value to our study because they provide a better representation of the blocking effect, a critical component to model the eastern warm and drier air masses. Lastly, it should be highlighted that the TC method presents a highly irregular surface which can bring more instability in a climate model.

Evaluation of the MAR

MAR underestimates annual mean temperatures and overestimates annual precipitation compared to CRU in our region of interest. These two results prove that MAR is not able to reproduce the warm and dry air masses at a resolution of 10 km. This can be partially explained by the fact that the standard generalization method used in MAR, the mean method, does not fully reproduce the mountain range. Finally, in our comparison between the 10 and 20 km output results, we observed that a higher spatial resolution can slightly improve mean temperature representation. Yet, there is still a significant bias not resolved in terms of precipitation modelling.

DEM generalization sensitivity experiments

Our results partially confirm our starting hypothesis. First, there is an increase in temperature for two out of three DEM generalization methods: P90 and TC methods. Meanwhile, the EM method produces a decrease in mean temperature because altitudes are too exaggerated compared to the mean method. Secondly, results in terms of precipitation are also in good agreements with our hypothesis for two out of three methods. As a matter of fact, the P90 and EM methods produce a significant decrease in precipitation in our region of interest, whereas the TC method induces no clear decrease in precipitation. This could be explained by the fact that the latter better represents the valleys at the expense of a perfect homogenisation of the mountain range. The air masses can therefore cross this irregular range and produce more precipitation. Furthermore, an increase in the instability can also affect precipitation modelling.

Conclusion

The results of our findings lead us to conclude that the P90 and EM generalization methods can better represent the warm and dry air masses thanks to a better mountain range representation. As a matter of fact, the surface elevation computed by these methods blocks cold and wet winds coming from the ocean and reproduces the typical Foehn winds descending to the lee of the Andes. Still, the EM method exaggerates the altitudes which is noticeable in the high negative temperature difference. The results obtained with the TC method are more difficult to interpret. On the one hand, the simulations produce an increase in mean temperatures which is the opposite of the underestimation displayed on the verification of MAR. On the other hand, the precipitation patterns do not resolve the bias observed in our evaluation of MAR.

In the end, we can draw the conclusion that none of these three methods are perfect. They obviously present different strengths and weaknesses at a given resolution of 10 km. The EM method is the most consistent at representing the mountain range and the blocking effect at the expense of a shortage of valleys and plains, causing a drop in the mean temperature. The TC method shows orographic features which are the closest to the original DEM. The method presents an accurate mean temperature representation at the expense of a reliable blocking effect mapping. Finally, the P90 method results in a good tradeoff with a fine representation of the mountain range allowing a more consistent air masses modelling. However, the mean temperature increase and precipitation decrease are not sufficient to cope with the biases observed with CRU.

This research can serve as a recommendation for a better use of DEM generalization to existing climate models performing in Patagonia but also in all regions where Foehn winds can be observed as well as in regions sharing the same orographic features as the Patagonian relief.

5.4 Perspectives

In the light of our study, we suggest a list of perspectives on this topic.

Firstly, our research was limited to the CRU gridded climate datasets to verify the standard performance of the model. A validation of this model could therefore be performed with other gridded climate datasets available in the region, but also with a meteorological station network analysis.

Secondly, following our conclusion, none of the trial DEM generalization methods as presented in our research is able to perfectly correct the bias observed in terms of precipitation and mean temperature. It would be interesting to investigate whether a 5 km spatial resolution combined with or without the different DEM generalization methods can correct the bias.

Finally, there is a dire need for better documentation, classification and use of the different DEM generalization methods in climate models, RCMs, and GCMs. The benefit and the value of this component are too often neglected in climatology and a more efficient use of it could lead to more consistent Foehn effects modelling and other climatic features, especially in complex orographic areas.

List of acronyms

CRU: Climate Research Unit

DEM: Digital Elevation Model

ECMWF: European Centre For Medium Range Weather Forecasting

EM: Envelope Maximum

GCM: General Climate Model

GFS: Global Forecast System

LGGE: Laboratoire de Glaciologie et Géophysique de l'Environnement

MAR: Modèle Atmosphérique Régional

NESTOR: NESTing Organization for the preparation of meteorological and surface fields in Regional models

NWS: United States' National Weather Service

P90: Percentile 90

RCM: Regional Climate Model

SISVAT: Soil Ice Snow Vegetation Atmosphere Transfer

TC: Thalwegs an crests

ULiège: University of Liège

Bibliography

Amante, C. and Eakings, B. (2009). Etopo1 1 arc-minute global relief model: procedures, data sources and analysis.

Andrew, O., Tony, P., Stuart, W., Andy, E., Mark, W., Scott, H., and John, T. (2014). Met office unified model high-resolution simulations of a strong wind event in antarctica. *Quarterly Journal of the Royal Meteorological Society*, 140(684):2287–2297. doi: 10.1002/qj.2296.

Barthélemy, A., Goosse, H., Mathiot, P., and Fichefet, T. (2012). Inclusion of a katabatic wind correction in a coarse-resolution global coupled climate model. *Ocean Modelling*, 48:45–54. doi: 10.1016/j.ocemod.2012.03.002.

Berman, A. L., Silvestri, G., and Compagnucci, R. (2012). Eastern patagonia seasonal precipitation: Influence of southern hemisphere circulation and links with subtropical south american precipitation. *Journal of Climate*, 25(19):6781–6795. doi: 10.1175/JCLI-D-11-00514.1.

Berman, A. L., Silvestri, G., and Compagnucci, R. (2013). On the variability of seasonal temperature in southern south america. *Climate dynamics*, 40(7-8):1863–1878. doi: 10.1007/s00382-012-1596-5.

Bian, L. and Butler, R. (1999). Comparing effects of aggregation methods on statistical and spatial properties of simulated spatial data. *Photogrammetric engineering and remote sensing*, 65:73–84. doi: 0099-1112/99/6501-0073$3.00.

Bianchi, E., Villalba, R., Viale, M., Couvreux, F., and Marticorena, R. (2016). New precipitation and temperature grids for northern patagonia: Advances in relation to global climate grids. *Journal of Meteorological Research*, 30(1):38–52. doi: 10.1007/s13351-015-5058-y.

Bindlish, R. and Barros, A. P. (1996). Aggregation of digital terrain data using a modified fractal interpolation scheme. *Computers & Geosciences*, 22(8):907–917. doi: 10.1016/S0098-3004(96)00049-0.

Carrasco, J. F., Casassa, G., and Rivera, A. (2002). Meteorological and climatological aspects of the southern patagonia icefield. In *The Patagonian Icefields*, pages 29–41. Springer. doi: 10.1007/978-1-4615-0645-4_4.

De Ridder, K. and Gallée, H. (1998). Land surface–induced regional climate change in southern israel. *Journal of Applied Meteorology*, 37(11):1470–1485. doi: 10.1175/1520-0450(1998)037<1470:LSIRCC>2.0.CO;2.

Dee, D. P., Uppala, S. M., Simmons, A., Berrisford, P., Poli, P., Kobayashi, S., Andrae, U., Balmaseda, M., Balsamo, G., Bauer, d. P., et al. (2011). The era-interim reanalysis: Configuration and performance of the data assimilation system. *Quarterly Journal of the royal meteorological society*, 137(656):553–597. doi: 10.1002/qj.828.

ECMWF (2003). Ifs documentation, part iv: Physical processes (cy25r1). *The Library ECMWF, Reading*.

Elvidge, A. D. and Renfrew, I. A. (2016). The causes of foehn warming in the lee of mountains. *Bulletin of the American Meteorological Society*, 97(3):455–466. doi: 10.1175/BAMS-D-14-00194.1.

Fettweis, X., Gallée, H., Lefebre, F., and Van Ypersele, J.-P. (2005). Greenland surface mass balance simulated by a regional climate model and comparison with satellite-derived data in 1990–1991. *Climate Dynamics*, 24(6):623–640. doi: 10.1007/s00382-005-0010-y.

Gallée, H. and Schayes, G. (1994). Development of a three-dimensional meso-γ primitive equation model: katabatic winds simulation in the area of terra nova bay, antarctica. *Monthly Weather Review*, 122(4):671–685. doi: 10.1175/1520-0493(1994)122<0671:DOATDM>2.0.CO;2.

Gallée, H., Fontaine de Ghélin, O., and van den Broeke, M. R. (1995). Simulation of atmospheric circulation during the gimex 91 experiment using a meso-γ primitive equations model. *Journal of Climate*, 8(11):2843–2859. doi: 10.1175/1520-0442(1995)008<2843:SOACDT>2.0.CO;2.

Gallée, H. and Pettré, P. (1998). Dynamical constraints on katabatic wind cessation in adélie land, antarctica. *Journal of the Atmospheric Sciences*, 55(10):1755–1770. doi: 10.1175/1520-0469(1998)055<1755:DCOKWC>2.0.CO;2.

Garreaud, R. (2009). The andes climate and weather. *Advances in Geosciences*, 22:3–11. doi: 10.5194/adgeo-22-3-2009.

Garreaud, R. (2013). Warm winter storms in central chile. *Journal of Hydrometeorology*, 14(5):1515–1534. doi: 10.1175/JHM-D-12-0135.1.

Garreaud, R., Lopez, P., Minvielle, M., and Rojas, M. (2013). Large-scale control on the patagonian climate. *Journal of Climate*, 26(1):215–230. doi: 10.1175/JCLI-D-12-00001.1.

George, T., Costas, D., and Christos, Z. (2012). Does dynamical downscaling introduce novel information in climate model simulations of precipitation change over a complex topography region? *International Journal of Climatology*, 32(10):1572–1578. doi: 10.1002/joc.2360.

Harris, I., Jones, P., Osborn, T., and Lister, D. (2014). Updated high-resolution grids of monthly climatic observations–the cru ts3. 10 dataset. *International Journal of Climatology*, 34(3):623–642. doi: 10.1002/joc.3711.

Hoinka, K. P. (1985). What is a foehn clearance? *Bulletin of the American Meteorological Society*, 66(9):1123–1132. doi: 10.1175/1520-0477(1985)066<1123:WIAFC>2.0.CO;2.

Hong, S.-Y. (1999). New global orography data sets. *Office note 424*.

Jacques-Coper, M., Brönnimann, S., Martius, O., Vera, C. S., and Cerne, S. B. (2015). Evidence for a modulation of the intraseasonal summer temperature in eastern patagonia by the madden-julian oscillation. *Journal of Geophysical Research: Atmospheres*, 120(15):7340–7357. doi: 10.1002/2014JD022924.

Kittel, C., Amory, C., Agosta, C., Delhasse, A., Huot, P.-V., Fichefet, T., and Fettweis, X. (2018). Sensitivity of the current antarctic surface mass balance to sea surface conditions using mar. doi: 10.5194/tc-2018-106.

Klink, K. (1995). Surface aggregation and subgrid-scale climate. *International journal of climatology*, 15(11):1219–1240. doi: 10.1002/joc.3370151104.

Lara, A., Villalba, R., Wolodarsky-Franke, A., Aravena, J. C., Luckman, B. H., and Cuq, E. (2005). Spatial and temporal variation in nothofagus pumilio growth at tree line along its latitudinal range (35 40'–55 s) in the chilean andes. *Journal of Biogeography*, 32(5):879–893. doi: 10.1111/j.1365-2699.2005.01191.x.

Le Coz, M., Delclaux, F., Genthon, P., and Favreau, G. (2009). Assessment of digital elevation model (dem) aggregation methods for hydrological modeling: Lake chad basin, africa. *Computers & Geosciences*, 35(8):1661–1670. doi: 10.1016/j.cageo.2008.07.009.

Lenaerts, J. T. M., van den Broeke, M. R., van Wessem, J. M., van de Berg, W. J., van Meijgaard, E., van Ulft, L. H., and Schaefer, M. (2014). Extreme precipitation and climate gradients in patagonia revealed by high-resolution regional atmospheric climate modeling. *Journal of Climate*, 27(12):4607–4621. doi: 10.1175/JCLI-D-13-00579.1.

Lenderink, G. and Lenderink, G. (2003). *Simulation of present-day climate in RACMO2: first results and model developments*. Koninklijk Nederlands Meteorologisch Instituut.

Lopez, P., Chevallier, P., Favier, V., Pouyaud, B., Ordenes, F., and Oerlemans, J. (2010). A regional view of fluctuations in glacier length in southern south america. *Global and Planetary Change*, 71(1):85–108. doi: 10.1016/j.gloplacha.2009.12.009.

Mathiot, P., Barnier, B., Gallée, H., Molines, J. M., Le Sommer, J., Juza, M., and Penduff, T. (2010). Introducing katabatic winds in global era40 fields to simulate their impacts on the southern ocean and sea-ice. *Ocean Modelling*, 35(3):146–160. doi: 10.1016/j.ocemod.2010.07.001.

Paruelo, J. M., Beltrán, A., Jobbagy, E., Sala, O. E., and Golluscio, R. A. (1998). The climate of patagonia: general patterns and controls on biotic processes. *Ecología Austral*, 8(2):85–101.

Quintana, J. and Aceituno, P. (2012). Changes in the rainfall regime along the extratropical west coast of south america (chile): 30-43º s. *Atmósfera*, 25(1):1–22.

Richner, H. and Hächler, P. (2013). Understanding and forecasting alpine foehn. In *Mountain Weather Research and Forecasting*, pages 219–260. Springer. doi: 10.1007/978-94-007-4098-3_4.

Scorer, R. (1978). Foehn fallacies. In *Environmental Aerodynamics*, pages 419–422. Ellis Horwood Publisher.

Seluchi, M. E., Norte, F. A., Satyamurty, P., and Chou, S. C. (2003). Analysis of three situations of the foehn effect over the andes (zonda wind) using the eta–cptec regional model. *Weather and forecasting*, 18(3):481–501. doi: 10.1175/1520-0434(2003)18<481: AOTSOT>2.0.CO;2.

Silvestri, G. E. and Vera, C. S. (2003). Antarctic oscillation signal on precipitation anomalies over southeastern south america. *Geophysical Research Letters*, 30(21). doi: 10.1029/ 2003GL018277.

Smith, R. B. and Evans, J. P. (2007). Orographic precipitation and water vapor fractionation over the southern andes. *Journal of Hydrometeorology*, 8(1):3–19. doi: 10.1175/JHM555. 1.

Solman, S. A., Sanchez, E., Samuelsson, P., da Rocha, R. P., Li, L., Marengo, J., Pessacg, N. L., Remedio, A., Chou, S., Berbery, H., et al. (2013). Evaluation of an ensemble of regional climate model simulations over south america driven by the era-interim reanalysis: model performance and uncertainties. *Climate Dynamics*, 41(5-6):1139–1157. doi: 10.1007/s00382-013-1667-2.

Viale, M. and Garreaud, R. (2015). Orographic effects of the subtropical and extratropical andes on upwind precipitating clouds. *Journal of Geophysical Research: Atmospheres*, 120(10):4962–4974. doi: 10.1002/2014JD023014.

Vieux, B. E. (1993). Dem aggregation and smoothing effects on surface runoff modeling. *Journal of Computing in Civil Engineering*, 7(3):310–338. doi: 10.1061/(ASCE) 0887-3801(1993)7:3(310).

Villarroel, C., Carrasco, J. F., Casassa, G., and Falvey, M. (2013). Modeling near-surface air temperature and precipitation using wrf with 5-km resolution in the northern patagonia icefield: A pilot simulation. *Int. J. Geosci*, 4:1193–1199. doi: 10.4236/ijg.2013.48113.

Wang, Y., Sen, O. L., and Wang, B. (2003). A highly resolved regional climate model (iprc-regcm) and its simulation of the 1998 severe precipitation event over china. part i: Model description and verification of simulation. *Journal of Climate*, 16(11):1721–1738. doi: 10.1175/1520-0442(2003)016<1721:AHRRCM>2.0.CO;2.

Wehner, M. F., Smith, R. L., Bala, G., and Duffy, P. (2010). The effect of horizontal resolution on simulation of very extreme us precipitation events in a global atmosphere model. *Climate dynamics*, 34(2-3):241–247. doi: 10.1007/s00382-009-0656-y.

Wilson, J. P. and Gallant, J. C. (2000). Digital terrain analysis. *Terrain analysis: principles and applications*, 6(12):1–27.

Wu, S., Li, J., and Huang, G. (2008). A study on dem-derived primary topographic attributes for hydrologic applications: Sensitivity to elevation data resolution. *Applied Geography*, 28(3):210–223. doi: 10.1016/j.apgeog.2008.02.006.